Armandojanni Petrucci Orefice

Linear stability analysis of Oldroyd-B fluids flow in pipes

Università degli Studi di Napoli
Dipartimento di Ingegneria Industriale

Scuola di dottorato in Ingegneria Aerospaziale,
Navale e della Qualità - XXVII ciclo

Tesi di dottorato in
Ingegneria Aerospaziale

Linear stability analysis of Oldroyd-B fluids flow in pipes

ARMANDOJANNI PETRUCCI OREFICE

Tutor:
Prof. Ing. Gennaro Coppola
Prof. Ing. Luigi de Luca

Coordinatore:
Prof. Ing. Luigi de Luca

Marzo 2015

ABSTRACT

The flow of non-Newtonian fluids has recently gained considerable importance because of its applications in various branches of science, engineering and technology: particularly in material processing, chemical and nuclear industries, geophysics, and bioengineering. The study of non-Newtonian fluids flow is also of significant interest in oil reservoir engineering.

The inadequacy of the Navier-Stokes equations in describing the dynamics of such complex fluids has led to the formulation of other mathematical models able to predict their behaviour. One of them is the Oldroyd-B fluid model that acquired a particular importance since it can be seen as a conjunction of two special cases: the classical Newtonian fluid and the elastic fluid described by the Upper Convected Maxwell model. Moreover it is able to well describe the dynamics of highly dilute polymer solutions, the so-called Boger's fluids.

The aim of this thesis is to investigate the linear stability of fluids described by the Oldroyd-B constitutive equation in cylindrical geometry from the point of view of modal and non-modal analysis. Note that only in recent years non-modal stability analysis of the flow of such kind of fluids, only in two-dimensional channel configuration, has been worked out since of its complexity that does not allow to apply in a straightforward way the classical non-modal analysis tools.

Detailed parametric analyses of Oldroyd-B fluids in annular pipe have been performed. This flow configuration has been chosen not only for its wider application in industrial process, but also because it represents an intermediate case between the channel and the Hagen-Poiseuille flow by varying the inner radius of the pipe.

This investigation has demonstrated the different behaviour of

Oldroyd-B fluid with respect to the classical Newtonian one, and the energy budget analysis of the disturbance energy amplification has allowed to highlight some interesting physical mechanism governing such fluids.

KEYWORDS: viscoelastic fluids, Oldroyd-B, linear stability, annular pipe flow.

PREFACE

This doctoral thesis is a theoretical/numerical work that deals with the linear stability analysis of Oldroyd-B fluids in cylindrical geometries. This study arose inside the FARO project (October 2012 - December 2014) carried out in conjunctions with other departments of the university and focused on the analysis of the non-Newtonian phenomena that appears on confined shear flows of viscoelastic fluids. The main advisor of this work is Professor Gennaro Coppola while Professor Luigi de Luca acts as co-advisor.

The work is subdivided as follows:

The first chapter is an introduction to the basic characteristics of viscoelastic fluids. It is aimed at giving a quick resume of the main concepts underlying the formulation of constitutive equations in order to provide a better understanding of the most important parameters governing the dynamics of dilute polymer solutions.

The second chapter is a description of the main tools used in the linear stability analysis. A particular attention has been given to the non-modal stability analysis and to the problems that arise in applying it to viscoelastic fluids.

The third chapter is devoted to the problem formulation, i.e. the description of the analyzed flow geometries and the development of an opportune numerical code.

The fourth chapter details the results obtained by the linear stability analysis.

The conclusions are reported in the last chapter where the main originalities of this work are highlighted.

Parts of the results here reported have been presented at the following conferences:

1. A. Petrucci Orefice, G. Coppola, L. de Luca - *Linear stability analysis of pipe Poiseuille flow for an Oldroyd-B fluid* • APS Division of Fluid Mechanics - 66th Annual Meeting, 24-26 November 2013, Pittsburgh, Pennsylvania, USA

2. A. Petrucci Orefice, G. Coppola, A. Orazzo, L. de Luca - *Linear stability of viscoelastic Poiseuille flows in cylindrical configurations* • 10th European Fluid Mechanics Conference, 14-18 September 2014, Copenhagen, Denmark

CONTENTS

LIST OF FIGURES

LIST OF TABLES

1

VISCOELASTIC FLUIDS

Viscoelastic fluids are mainly suspensions of long-chain polymer molecules in a solvent. Adding polymers in a Newtonian solvent significantly varies its rheological properties even if the concentration is very small. The fluid changes and becomes non-Newtonian.

The term non-Newtonian fluid is an all-encompassing term denoting any fluid that does not obey to the Newton's law for the shear stress. This definition indicates just how these complex fluids *do not* behave, but in fact many new effects appear and have to be considered to define a suitable law[1] for the stress tensor.

[1] constitutive equation

One approach for defining a constitutive equation is to postulate a model for the microstructure then explore the consequences on the macroscopic level.[2] This viewpoint, which is opposed in some ways to the pure continuum approach,[3] has been preferred in recent times because gives more insights into the physical mechanisms underlying the non-Newtonian phenomena. Moreover it allows for an iterative process in which macroscopical effects excluded by simpler model can be added with subsequent revisitations of the representation of the microscopic structures.

Many authors[4] seem to agree with the fact that the microscopic approach has to be always preferred even by who wants just to deal with the effects related to the larger scales, because they inevitably depend on what happens to the molecular structure.
Bird and Wiest expressly stated about this matter that

[2] N. Phan-Thien (2012). *Understanding Viscoelasticity*. Springer.

[3] see J. G. Oldroyd (1950). "On the Formulation of Rheological Equations of State". In: *Proceedings of the Royal Society of London A: Mathematical, Physical and Engineering Sciences* 200.1063, pp. 523–541.

[4] e.g. see R. B. Bird and J. M. Wiest (1995). "Constitutive equations for polymeric liquids". In: *Annual review of fluid mechanics* 27.1, pp. 169–193; J. M. Rallison and E. J. Hinch (1988). "Do we understand the physics in the constitutive equation?" In: *Journal of Non-Newtonian Fluid Mechanics* 29, pp. 37–55.

"The importance of molecular viewpoint cannot be overlooked, and the fluid dynamicist who fails to take cognizance of the advances in kinetic theory limits his ability to solve problems."

SIMPLE MOLECULAR MODELS

Polymers are macromolecules organized as chains of monomers that in equilibrium tend *naturally* to curl up for probabilistic reasons due to the fact that fewer configurations are available in an extended conformation . Because of the Brownian forces they do not actually stand in a single configuration but *explore* different equiprobable ones while retaining the same average dimension. This state is the so called *random coil* and happens in dilute polymer solutions, in which contacts between polymers are negligible and interactions with the solvent are predominant.

In some peculiar conditions, i.e. if the solvent is not a *good* solvent for the polymer and is at the so called *θ-temperature*, the polymer macromolecule can be modeled with a freely rotating chain with N segments, the *ideal chain* or *Kramer chain*. Its segments are called *statistical monomers* or *Khun segments* and do not correspond to the actual monomers of the polymer chain nor are physical entities, i.e. they are freely rotating irrespective of the neighbouring segments and can cross each other without any limitation.[5]

In this hypothesis the chain is completely equivalent to the *random walk* mathematical model for which the end-to-end vector is

$$R = \sum_{j=1}^{N} R_j \qquad (1.1)$$

On the average the randomly oriented vector will have zero mean

$$\langle R_j \rangle = 0 \qquad (1.2)$$

$$\langle R_i \cdot R_j \rangle = \begin{cases} 0 & \text{if} \quad i \neq j \\ b^2 & \text{if} \quad i = j \end{cases} \qquad (1.3)$$

where the angular brackets denote the average with respect to the probability density function of the considered variable. Thus it has

good solvent   interacts favourably with the polymer, leading to an expanded chain configuration.

θ-temperature   is the temperature at which the attractive and repulsive forces of mutual interaction of the monomers are compensated. A solvent at this temperature is also called a *θ-solvent*.

For the sake of completeness it has to be pointed out that much more detailed chain models would consider the fact that, because of the chemical bonds, the angle of rotation between two successive segments is actually quite narrow. (P. J. Flory [1969]. *Statistical mechanics of chain molecules*. Wiley-Interscience)

[5] Phan-Thien, *Understanding Viscoelasticity*.
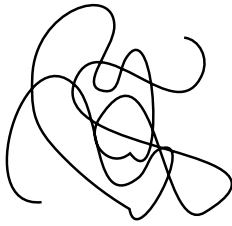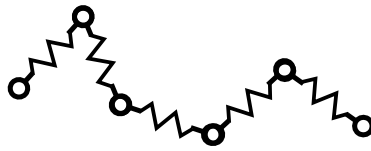
Random coil   Rouse model   Dumbbell model

Figure 1.1: Schemes of simple molecular models

zero end-to-end vector on average

$$\langle \boldsymbol{R} \rangle = \sum_{j=1}^{N} \langle \boldsymbol{R}_j \rangle = \boldsymbol{0} \qquad (1.4)$$

while the average dimension will be

$$\langle R^2 \rangle = \langle \boldsymbol{R} \cdot \boldsymbol{R} \rangle = Nb^2 \qquad (1.5)$$

Elastic dumbbell model

The most important model that describes the dynamics of the ideal chain is the *Rouse model*. The forces are schematized associating a point mass, i.e. a bead, and a spring with each Khun segment. The *Zimm model* is an extension that includes hydrodynamic interactions.

The elastic dumbbell model is a simplification of the Rouse model in which the polymer macromolecule is described by only two beads and a connecting spring (Figure 1.1). It is a quite crude model that does not describe any detail of the molecular architecture at all and is quite inadequate for chemists interested in the kinetic theory approach.[6]

Nevertheless, it captures some important features of dilute polymer solutions. The dumbbell can rotate and stretch because of the flow and the elastic behaviour can describe the slowest, and in some extent also the most important, motion of the polymer chain, i.e. the deformation of the entire macromolecule. These aspects make it suitable at least for

[6] R.B. Bird et al. (1987b). *Dynamics of Polymeric Liquids. Kinetic Theory*. Second Edition. Vol. II. Wiley-Iterscience.

the qualitative description of many effects on the dynamics of dilute polymer solutions.

THE FORCES ACTING ON EACH BEAD are mainly three and can be subdivided as follows, while neglecting external forces, such as gravitational or electric ones, and hydrodynamic interactions:

Hydrodynamic drag force   is the resistance of the bead moving through the solution. The Reynolds number related to this effect is small because of the size of the polymer, thus the average motion of the chain is modeled with the Stokes' law and the frictional coefficient $\zeta = 6\pi\mu_s a$ is introduced, where a represent the bead radius and μ_s is the viscosity of the solvent.

$$F_d = \frac{1}{2}\zeta(\dot{R} - R \cdot \nabla V) \qquad (1.6)$$

Brownian force   acts on the bead because of the thermal fluctuations. An expression of this force can be obtained using the configurational distribution function, ψ,

$$F_B = k_B T \frac{\partial \ln \psi}{\partial R} \qquad (1.7)$$

where T is the temperature and k_B is the Boltzmann's constant.

Intramolecular force   is the elastic spring force that acts on the two beads. The choice of the law governing the behaviour of the spring is crucial for gaining accurate constitutive equations that are able to match the experimental data. Assuming a *Gaussian chain*,[7] modelled with the Hooke's law

$$F_e = HR \qquad (1.8)$$

where $H = \frac{3k_B}{Nb^2}$ is the constant spring stiffness, gives rise to the *linear elastic dumbbell* model. This assumption seems to be fair until the extension of the spring is below one third of the characteristic dimension of the polymer chain.[8]

[7] R. G. Larson (1999). *The Structure and Rheology of Complex fluids*. Oxford University Press, New York.

[8] Larson, op. cit.

OLDROYD-B CONSTITUTIVE EQUATION

The definition of a constitutive equation is necessary for expressing the behaviour of the tensor stress that will be used in the momentum

balance equation. The Oldroyd-B model[9] is among the simplest differential constitutive equations.[10] It is a 2-constants variant of the 8-constants constitutive equations proposed by Oldroyd in 1950. The derivation of the complete model is based on considerations on the foundational mathematical aspects that a constitutive equations should respect.

While it has been originally developed from a continuum point of view, the B version can be derived also by the dumbbell model described before. The dilute polymer solution is then modelled as a dispersion of dumbbells in the Newtonian solvent. The interpretation from the two points of view, along with its almost simple analytical formulation, makes it a suitable tool for a deeper understanding of the macroscopic viscoelastic effects on the flows.

Solving for $\dot{R}$ the balance of the three forces, expressed by equations (1.6), (1.7) and (1.8), acting on the dumbbell

$$\frac{1}{2}\zeta(\dot{R} - R \cdot \nabla V) + HR + k_B T\frac{\partial \ln \psi}{\partial R} = 0 \tag{1.9}$$

and inserting the result in a probability balance equation

$$\frac{\partial \psi}{\partial t} + \frac{\partial}{\partial R} \cdot (\dot{R}\psi) = 0 \tag{1.10}$$

gives the *Fokker-Planck* or *Smoluchowski equation* that reads

$$\frac{\partial \psi}{\partial t} + \frac{\partial}{\partial R} \cdot \left[R \cdot \nabla V\psi - \frac{2k_B T}{\zeta}\frac{\partial \psi}{\partial R} - \frac{2H}{\zeta}R\psi \right] = 0 \tag{1.11}$$

The equation governing the evolution of the *conformation tensor* $\langle RR \rangle$ can be obtained integrating over the R coordinates

$$\frac{\partial \langle RR \rangle}{\partial t} - \nabla V^{\mathrm{T}} \cdot \langle RR \rangle - \langle RR \rangle \cdot \nabla V + \frac{4H}{\zeta}\langle RR \rangle - \frac{4k_b}{\zeta}\mathsf{I} = 0 \tag{1.12}$$

This equation can be rearranged as

$$\langle RR \rangle + \lambda \left\{ \frac{\partial \langle RR \rangle}{\partial t} - \nabla V^{\mathrm{T}} \cdot \langle RR \rangle - \langle RR \rangle \cdot \nabla V \right\} = \frac{1}{3}Nb^2\mathsf{I} \tag{1.13}$$

introducing the *Rouse relaxation time*

$$\lambda = \frac{\zeta}{4H} = \frac{\zeta Nb^2}{12k_B T}. \tag{1.14}$$

The term in parenthesis is the *upper-convected derivative* of the conformation tensor. In general the upper-convected derivative of a tensor is

$$\frac{\delta\bullet}{\delta t} = \frac{\partial\bullet}{\partial t} - \nabla V^{\mathrm{T}} \cdot \bullet - \bullet \cdot \nabla V$$

The evolution of the polymer-contributed stress $\boldsymbol{\sigma}_\mathrm{p} = \nu H \langle \boldsymbol{RR} \rangle$, where ν is the concentration of dumbbells in the volume unit, can be obtained by multiplying (1.13) by νH

$$\boldsymbol{\sigma}_\mathrm{p} + \lambda \left\{ \frac{\partial \boldsymbol{\sigma}_\mathrm{p}}{\partial t} - \nabla V^\mathrm{T} \cdot \boldsymbol{\sigma}_\mathrm{p} - \boldsymbol{\sigma}_\mathrm{p} \cdot \nabla V \right\} = G\mathsf{I} \qquad (1.15)$$

where

$$G = \frac{1}{3} N b^2 \nu H = \nu k_\mathrm{B} T. \qquad (1.16)$$

The stress tensor due to the polymer contribution can be also rearranged as

$$\boldsymbol{\tau}_\mathrm{p} = \boldsymbol{\sigma}_\mathrm{p} - G\mathsf{I} \qquad (1.17)$$

Since $\boldsymbol{\sigma}_\mathrm{p}$ is proportional to $\langle \boldsymbol{RR} \rangle$ is positive definite while $\boldsymbol{\tau}_\mathrm{p}$ is not.

obtaining from (1.15)

$$\boldsymbol{\tau}_\mathrm{p} + \lambda \left\{ \frac{\partial \boldsymbol{\tau}_\mathrm{p}}{\partial t} - \nabla V^\mathrm{T} \cdot \boldsymbol{\tau}_\mathrm{p} - \boldsymbol{\tau}_\mathrm{p} \cdot \nabla V \right\} = 2\mu_\mathrm{p} \mathsf{D} \qquad (1.18)$$

where $\mathsf{D} = (\nabla V + \nabla V^\mathrm{T})/2$ and

$$\mu_\mathrm{p} = G\lambda = \frac{\nu \zeta N b^2}{12} = \frac{1}{2} \pi \nu a N b^2 \mu_\mathrm{s} \qquad (1.19)$$

is the polymer-contributed viscosity.

THE OLDROYD-B MODEL is obtained considering that, for a dilute solution of dumbbells, the contribution to the stress due to the Newtonian solvent $\boldsymbol{\tau}_\mathrm{s} = 2\mu_\mathrm{s} \mathsf{D}$ can not be overlooked. Adding $\boldsymbol{\tau}_\mathrm{s}$ to $\boldsymbol{\tau}_\mathrm{p}$ and considering equation (1.18) gives

$$\boldsymbol{\tau} + \lambda_1 \frac{\delta \boldsymbol{\tau}}{\delta t} = 2\mu \left(\mathsf{D} + \lambda_2 \frac{\delta \mathsf{D}}{\delta t} \right) \qquad (1.20)$$

where λ_1 and λ_2 are the two constants of the Oldroyd-B model and are respectively the *relaxation time*, λ, and the *retardation time*, $\lambda \mu_\mathrm{s}/\mu$. The *total viscosity* is the sum of the solvent viscosity and the polymer-contributed one

$$\mu = \mu_\mathrm{s} + \mu_\mathrm{p} \qquad (1.21)$$

The *total stress tensor* can be written analogously as

$$\boldsymbol{\pi} = -p\mathsf{I} + \boldsymbol{\tau}_\mathrm{s} + \boldsymbol{\tau}_\mathrm{p} \qquad (1.22)$$

where the pressure is the sum of the solvent and polymer contribution, $p = p_\mathrm{s} + p_\mathrm{p}$.[11] A rearrangement of the previous equation can be

[11] Bird et al., *Dynamics of Polymeric Liquids*.

obtained including all the isotropic terms in the pressure

$$\boldsymbol{\pi} = -p_{\mathrm{T}}\mathbf{I} + \boldsymbol{\tau}_{\mathrm{s}} + \boldsymbol{\sigma}_{\mathrm{p}}. \qquad (1.23)$$

This model can be seen as intermediate between the Newtonian law and the Upper Convected Maxwell model. Indeed for $\mu_{\mathrm{s}} = 0$ the retardation time is zero, $\lambda_2 = 0$, and the total viscosity is equivalent to the polymer related one, thus equation (1.18) is recovered. The Newtonian limit can be obtained in two different ways

$\mu_{\mathrm{p}} = 0$ that implies that the total viscosity is equivalent to the solvent one and also that the retardation time is equal to the to relaxation one, $\lambda_2 = \lambda_1 = \lambda$

$\lambda = 0$ thus $\lambda_2 = 0$ again but this time the contribution of the polymer to the stress is not zero. It just acts as the Newtonian component, i.e. with relaxation time equal to zero.

Some unphysical aspects can limit the use of the Oldroyd-B model; these are given essentially by the fact that the spring has not limits to its extendibility, i.e. the polymer can become infinite. For this reason the model predicts an infinite stress for finite elongational rate of $1/(2\lambda)$. Constitutive equations such as FENE (Finitely Extensibile Nonlinear Elasitc) models limits the maximum extensibility of the polymer and overcome this kind of drawback. This is made by multiplying $\boldsymbol{\tau}_{\mathrm{p}}$, defined by equation (1.17), for a suitable function. One common choice is the Peterlin's closure function that leads to the FENE-P model. Another way of resolving this unwanted behaviour is to insert non-linear terms in equation (1.18). An example of this kind of approach is the *Giesekus* constitutive equation.[12]

The Oldroyd-B model exhibits another unlike but at the same time interesting behaviour. It predicts constant viscosity for steady state shear flows.

The independence of the viscosity by the shear rate seems to be not such restrictive but in fact it is quite untypical for the majority of the polymer solutions that are inherently shear-thinning.

There is however a class of fluids, the *Boger's fluids*, that are dilute polymer solutions, so dilute that the variation of viscosity with shear rate can be ignored.[13] The viscosity of the solvent is then so predominant that the total viscosity is independent of shear rate or nearly so.

[12] H. Giesekus (1982). "A simple constitutive equation for polymer fluids based on the concept of deformation-dependent tensorial mobility". In: *Journal of Non-Newtonian Fluid Mechanics* 11.1, pp. 69–109.

BOGER'S FLUIDS

[13] D. F. James (2009). "Boger Fluids". In: *Annual review of fluid mechanics* 41, pp. 129–142.

The introduction of this type of fluids has been important in separating the purely elastic effects from the viscous ones in non-Newtonian flows because the viscous ones can be determined with the Newtonian fluids.

GOVERNING EQUATIONS

The governing equations for the incompressible flow of Oldroyd-B fluids are given by the continuity equation

$$\rho \, \nabla \cdot V = 0, \tag{1.24}$$

and the momentum balance

$$\rho \frac{\partial V}{\partial t} + \rho V \cdot \nabla V = \nabla \cdot \boldsymbol{\pi}. \tag{1.25}$$

An equation related to the evolution of the polymeric stress tensor, i.e. an equation chosen between (1.13),(1.15) and (1.18), has to be added to close the problem. The total stress tensor is given by equation (1.22), where the polymer stress tensor can be rewritten taking into account equations (1.16) and (1.19) as

$$\boldsymbol{\tau}_{\mathrm{p}} = \frac{\mu_{\mathrm{p}}}{\lambda} \left(\frac{\boldsymbol{\sigma}_{\mathrm{p}}}{G} - \mathbf{I} \right) = \frac{\mu_{\mathrm{p}}}{\lambda} \left(\frac{H}{k_{\mathrm{B}} T} \langle RR \rangle - \mathbf{I} \right) \tag{1.26}$$

The momentum balance can be then rearranged as

$$\rho \frac{\partial V}{\partial t} + \rho V \cdot \nabla V + \nabla p = \mu_{\mathrm{s}} \, \nabla^2 V + \frac{\mu_{\mathrm{p}}}{\lambda} \, \nabla \cdot \left(\frac{H}{k_{\mathrm{B}} T} \langle RR \rangle - \mathbf{I} \right) \tag{1.27}$$

THE DIMENSIONLESS EQUATIONS are

$$\nabla \cdot U = 0 \tag{1.28}$$

$$\frac{\partial U}{\partial t} + U \cdot \nabla U + \nabla p = \frac{\beta}{\mathcal{R}e} \nabla^2 U + \frac{1 - \beta}{\mathcal{R}e} \nabla \cdot \mathbf{t}_{\mathrm{p}} \tag{1.29}$$

and can be obtained by introducing the *Reynolds number* $\mathcal{R}e = \rho \mathcal{U} l / \mu$ where $\mathcal{U}$ and l represent appropriate choices of velocity and length scales for the problem under investigation, while μ is the total viscosity of the polymeric solution. The dimensionless number $\beta = \mu_{\mathrm{s}} / \mu$ is the *viscosity ratio* and can be seen as a measure of the polymer concentration in the solution; for $\beta = 1$ the Newtonian case is

recovered while decreasing it the amount of polymer increases until $\beta = 0$ and the Upper Convected Maxwell model is reached.

The dimensionless polymer stress tensor $\mathbf{t}_\mathrm{p}$ is obtained by taking into account equation (1.26) and non-dimensionalizing $\langle RR \rangle$ by $k_\mathrm{B}T/H$

$$\mathbf{t}_\mathrm{p} = -\frac{(\mathbf{I} - \mathbf{C})}{\mathcal{W}i} \tag{1.30}$$

where the *Weissenberg number* $\mathcal{W}i = \lambda\, \mathcal{U}/l$ is the product of the polymer relaxation time λ and the rate of strain $\mathcal{U}/l$. When $\mathcal{W}i \to 0$ also the polymer relaxation time tends to zero, thus the Newtonian limit is recovered again.

The evolution of the dimensionless conformation tensor $\mathbf{C}$ is obtained by equation (1.13) and reads

$$\frac{\partial \mathbf{C}}{\partial t} + U \cdot \nabla \mathbf{C} = \mathbf{C} \cdot \nabla U + (\nabla U)^\mathrm{T} \cdot \mathbf{C} + \frac{(\mathbf{I} - \mathbf{C})}{\mathcal{W}i}. \tag{1.31}$$

2

LINEAR STABILITY

Starting from a steady state solution $\overline{Q}$ of the set of governing differential equations, presented in the previous Chapter, an infinitesimal disturbance q is added so that the perturbed vector of state becomes

$$Q = \overline{Q} + q. \qquad (2.1)$$

The evolution of the disturbance is obtained by subtracting the steady state equation from the complete set of non-stationary governing equations of the perturbed quantity; linearization is then applied neglecting all the quadratic perturbation terms and leads to

$$\frac{\partial}{\partial t} q = \mathcal{L}q \qquad (2.2)$$

where $\mathcal{L}$ is the spatial differential operator. The discretization of this equation leads to

$$\frac{\partial}{\partial t} q = \mathbf{L}q \qquad (2.3)$$

Modal stability analysis is obtained applying the temporal normal mode position, i.e.

$$q = q^\circ \, e^{-i\omega t} \qquad (2.4)$$

and leads to the following eigenvalue problem

$$-i\omega q = \mathbf{L}q \qquad (2.5)$$

where the imaginary part of ω gives informations on the asymptotic behaviour of the disturbance, i.e. if $\omega_i < 0$ the modal disturbance is stable.

NON-MODAL STABILITY ANALYSIS captures the transient behaviour of the disturbances. The problem is changed to an initial value problem. It has been demonstrated that even in subcritical modal conditions some initial disturbances may experience an amplification during in the short time of the evolution before decaying. This effect has been proven to be due to the non-normality of the linearized differential operator[1] thus the name of non-modal stability analysis.

The solution of the linearized problem expressed by equation (2.2) can be written as

$$e^{\mathbf{L}t}\boldsymbol{q}_0 = \boldsymbol{q} \tag{2.6}$$

where $\boldsymbol{q}$ is the generic vector of state at the time t while $\boldsymbol{q}_0$ is the initial condition, i.e. $\boldsymbol{q}$ at the time $t = 0$.

The definition of a suitable norm to use for measuring the vector of state is one of the most important aspects in order to proceed with the non-modal analysis and compute the transient growth.[2] In fact the appearance of the transient amplification depends on how it is measured, i.e. with some norms the transient growth may not exist. Moreover also the physical meaning of the transient growth depends on the chosen norm.

In the case of incompressible flow of Newtonian fluids the state vector is the velocity vector and the total energy, i.e. the kinetic energy, is given by

$$E = \int_{\Omega} \boldsymbol{q}^{\mathrm{T}}\mathbf{M}\boldsymbol{q}\,\mathrm{d}V \tag{2.7}$$

and naturally induce an energy norm and an inner product. The amplification of such a norm is easily understandable as an amplification of the kinetic energy of the flow field. Moreover its equivalence with the Euclidean norm can be obtained by the following equation

$$\|\boldsymbol{q}\|_E = \|\mathbf{F}\boldsymbol{q}\|_2 \tag{2.8}$$

where $\mathbf{F}$ is obtained by the Cholesky decomposition, $\mathbf{M} = \mathbf{F}^{\mathrm{T}}\mathbf{F}$, of the symmetric positive-definite weight matrix $\mathbf{M}$.

THE TRANSIENT GROWTH FUNCTION is thus the induced norm of the operator defined by equation (2.6)

$$G(t) = \max\frac{\|\boldsymbol{q}\|_E}{\|\boldsymbol{q}_0\|_E} = \max\frac{\|\mathbf{F}\boldsymbol{q}\|_2}{\|\mathbf{F}\boldsymbol{q}_0\|_2} = \max\frac{\|\mathbf{F}\,e^{\mathbf{L}t}\boldsymbol{q}_0\|_2}{\|\mathbf{F}\boldsymbol{q}_0\|_2} = \max\|\mathbf{F}\,e^{\mathbf{L}t}\,\mathbf{F}^{-1}\|_2 \tag{2.9}$$

[1] see L. N. Trefethen and M. Embree (2005). *Spectra and pseudospectra: the behavior of nonnormal matrices and operators*. Princeton University Press, pp. xviii + 606; P. J. Schmid and D. S. Henningson (2001). *Stability and transition in shear flow*. Springer.

[2] P. J. Schmid (2007). "Nonmodal Stability Theory". In: *Annu. Rev. Fluid Mech.* 39, pp. 129–162.

It gives the maximum amplification obtainable at a certain time considering all the possible initial conditions. This implies that for two different instants the initial disturbance that reaches the maximum amplification may be different.

Changing even slightly the problem, for example dealing with compressible flows of Newtonian fluids,[3] the definition of a scalar product and associated norm becomes not so obvious, but it is anyway possible to define a suitable norm for the vector of state that is expression of the the total energy.

[3] see A. Hanifi et al. (1996). "Transient growth in compressible boundary layer flow". In: *Physics of Fluids* 8.3, pp. 826–837.

THE PROBLEM OF NON-MODAL ANALYSIS FOR VISCOEALSTIC FLUIDS

In the particular case of incompressible flows of viscoelasitc fluids, the total energy is sum of the kinetic energy and of the elastic energy of polymers. An estimate of the contribution to the total energy related to the conformation tensor is given by Lozinski and Owens.[4] However the polymer contribution does not induce a natural norm for the conformation tensor[5] as it happens for the kinetic energy and the velocity vector in the Newtonian case of incompressible flows. Moreover the space of the symmetric positive-definite conformation tensors is not even a linear vector space.

[4] see A. Lozinski and R. G. Owens (2003). "An energy estimate for the Oldroyd B model: theory and applications". In: *Journal of Non-Newtonian Fluid Mechanics* 112.2, pp. 161–176.

[5] C. R. Doering et al. (2006). "Failure of energy stability in Oldroyd-B fluids at arbitrarily low Reynolds numbers". In: *Journal of Non-Newtonian Fluid Mechanics* 135.2, pp. 92–96.

On the other hand it is anyway possible to define a norm for the conformation tensor, e.g. the Frobenius norm, but it will be difficult to give physical interpretations to the results. These considerations make impossible the use of the transient growth tool for the non-modal analysis in a straightforward way.

An idea that seems suitable for overcoming the problems stated above would be to change the polymer variable from the conformation tensor to its unique positive definite square root. This change has been proposed for simulative purposes and a complete evolution equation of this tensor has been written.[6]
One of the main advantages of this formulation is that the scalar product of the square root of the conformation tensor gives the elastic energy associated to the polymer. However the spectral characteristics of this differential operator would be different from the ones of the set of equations related to the conformation tensor. It is sufficient to bear in mind that the relation between the conformation tensor and its

[6] N. Balci et al. (2011). "Symmetric factorization of the conformation tensor in viscoelastic fluid models". In: *Journal of Non-Newtonian Fluid Mechanics* 166.11, pp. 546–553.

square root is not linear. This fact should not limit the usage of such set of equations for the linear stability analysis of Oldroyd-B fluids flows but its suitability has not been investigated yet.

Non-modal analysis with filters

Only in recent times works on linear stability analysis of the channel flow of viscoelastic fluids started to deal with non-modal effects and many ideas have been proposed for facing the problems stated above for both inertial[7] and inertialess[8] cases. These authors tackle the non-modal stability problem using an *input-output* stochastic approach.

Another interesting approach is to focus only on the kinetic part of the total energy.[9] This idea is based on the fact that a fluid dynamicist is interested in what happens to the flow field. This is also the one that can be perturbed and monitored in laboratory during the experiments, thus also in performing the linear stability non-modal analysis it is supposed to perturb only the kinetic part of q and to monitor the evolution of the velocity field only.

The generalization of this approach is to give the possibility to perturb only one part of the vector of state and to monitoring the evolution of another one. This can be made by introducing two rectangular matrices, $\mathbf{B}$ and $\mathbf{P}$, defined to obtain the *filtered* vectors of state $q_{in} = \mathbf{B}q_0$ and $q_{out} = \mathbf{P}q$. As exemplifying case suppose to deal with the incompressible flow of a Newtonian fluid for which the vector of state is the velocity vector $q = [u, v, w]^{T}$ and to be interested in perturbing the v and w components, thus $q_{in} = [v, w]^{T}$ and in seeing how it affects the u and v components, thus $q_{out} = [u, v]^{T}$. In this case the filter matrices will be

$$\mathbf{B} = \begin{bmatrix} 0 & 1 & 0 \\ 0 & 0 & 1 \end{bmatrix}$$

$$\mathbf{P} = \begin{bmatrix} 1 & 0 & 0 \\ 0 & 1 & 0 \end{bmatrix}.$$

The projection q_{in} and q_{out} onto the original space of the complete vector of state could be done by using $\mathbf{B}^{T}$ and $\mathbf{P}^{T}$. It has to be stressed that this is not the inverse of the previous operation, i.e. if $q_{in} = \mathbf{B}q_0$, in general

$$q_0 \neq q_{0in} = \mathbf{B}^{T}q_{in} = \mathbf{B}^{T}\mathbf{B}q_0 \qquad (2.10)$$

[7] see Hoda et al. "Energy amplification in channel flows of viscoelastic fluids" (2008) and "Frequency responses of streamwise-constant perturbations in channel flows of Oldroyd-B fluids" (2009); and also see Jovanović and Kumar "Nonmodal amplification of stochastic disturbances in strongly elastic channel flows" (2011)

[8] see M. R. Jovanović and S. Kumar (2010). "Transient growth without inertia". In: *Physics of Fluids* 22.2, p. 023101.

[9] M. Zhang et al. (2013). "Linear stability analysis of channel flow of viscoelastic Oldroyd-B and FENE-P fluids". In: *Journal of Fluid Mechanics* 737, pp. 249–279.

For the particular case of being interested in the same part of the vector of state for both the perturbation and the evolution, e.g. in the same components of the velocity vector, then $\mathbf{P} = \mathbf{B}$.

For the previous example it is trivial to see that $\boldsymbol{q}_{0\text{in}} = [0, v_0, w_0]$ is not equal to $\boldsymbol{q}_0$ that can have any value for the u component.

Only for the subset of $\boldsymbol{q}_{0\text{in}}$ operations such as **B** are bijective. The main idea is then to evolve *only* the subset of vectors $\boldsymbol{q}_{0\text{in}}$, i. e. vectors with

- non zero components homologous to $\boldsymbol{q}_{\text{in}}$

- other components equal to zero

Figure 2.1: Operation **B** is not bijective.

Evolving this subset will individuate another subset in the codomain of the evolved vectors $\boldsymbol{q}$. In general the evolved vectors will not have zero values in the components non homologous to $\boldsymbol{q}_{\text{in}}$ but it possible anyway to decide to *monitor* only *some* of the components of the evolved vector by using the filter matrix **P**.

$$\mathbf{P}\, e^{\mathbf{L}t}\mathbf{B}^{\mathsf{T}}\boldsymbol{q}_{\text{in}} = \boldsymbol{q}_{\text{out}} \tag{2.11}$$

is the evolution of the chosen components of the vector of state, $\boldsymbol{q}_{\text{out}}$ starting by an initial condition of $\boldsymbol{q}_{0\text{in}} = \mathbf{B}^{\mathsf{T}}\boldsymbol{q}_{\text{in}}$, where components not homologous to $\boldsymbol{q}_{\text{in}}$ are zero. The energy associated to $\boldsymbol{q}_{\text{in}}$ and $\boldsymbol{q}_{\text{out}}$ can be written as

$$E_{\text{in}} = \int_V \boldsymbol{q}_{\text{in}}^{\mathsf{T}}\mathbf{M}_{\text{in}}\boldsymbol{q}_{\text{in}}\mathrm{d}V \tag{2.12}$$

$$E_{\text{out}} = \int_V \boldsymbol{q}_{\text{out}}^{\mathsf{T}}\mathbf{M}_{\text{out}}\boldsymbol{q}_{\text{out}}\mathrm{d}V \tag{2.13}$$

THE TRANSIENT GROWTH FUNCTION with *filters* matrices will be then

$$G(t) = \max \frac{\|\boldsymbol{q}_{\text{out}}\|_{E_{\text{out}}}}{\|\boldsymbol{q}_{\text{in}}\|_{E_{\text{in}}}} = \max \frac{\|\mathbf{F}_{\text{out}}\boldsymbol{q}_{\text{out}}\|_2}{\|\mathbf{F}_{\text{in}}\boldsymbol{q}_{\text{in}}\|_2} = \max \frac{\|\mathbf{F}_{\text{out}}\,\mathbf{P}\,e^{\mathbf{L}t}\mathbf{B}^{\mathsf{T}}\boldsymbol{q}_{\text{in}}\|_2}{\|\mathbf{F}_{\text{in}}\boldsymbol{q}_{\text{in}}\|_2} =$$

$$= \max \frac{\|\mathbf{F}_{\text{out}}\,\mathbf{P}\,e^{\mathbf{L}t}\mathbf{B}^{\mathsf{T}}\boldsymbol{q}_{\text{in}}\|_2}{\|\mathbf{F}_{\text{in}}\boldsymbol{q}_{\text{in}}\|_2} = \max \|\mathbf{F}_{\text{out}}\,\mathbf{P}\,e^{\mathbf{L}t}\,\mathbf{B}^{\mathsf{T}}\mathbf{F}_{\text{in}}^{-1}\|_2 \tag{2.14}$$

PROJECTION ONTO THE EIGENVECTORS BASIS

For many reasons of computational costs and accuracy of the solution it is possible to make a projection of the state vector onto the basis of the eigenvectors of the linear differential operator **L**

$$\boldsymbol{q} = \mathbf{S}k$$

where $\mathbf{S}$ is the matrix of the eigenvectors (columns) of $\mathbf{L}$ and k is the vector of the contravariant components of q with respect of this basis. If this basis is complete, thus the eigenvectors are linearly independent, then equation (2.6) can be easily diagonalized obtaining

$$e^{\Lambda t} k_0 = k \qquad (2.15)$$

where Λ is the diagonal matrix of the eigenvalues of $\mathbf{L}$. Substituting in the definition of the energy

$$E = \int_\Omega k^T \, \mathbf{S}^T \mathbf{M} \mathbf{S} \, k \, \mathrm{d}V \qquad (2.16)$$

and being $k = k(t)$, i.e. it is function of the time only,

$$E = k^T \int_\Omega \mathbf{S}^T \mathbf{M} \mathbf{S} \, \mathrm{d}V \, k \qquad (2.17)$$

and to define the matrix of inner products of the eigenvectors

$$M = \int_\Omega \mathbf{S}^T \mathbf{M} \mathbf{S} \, \mathrm{d}V \qquad (2.18)$$

M is called Gramian (see Schmid and Henningson) and is not equal to the weight matrix $\mathbf{M}$ thus $F \neq \mathbf{F}$.

that can be decomposed as $M = F^T F$ because is symmetric and positive-definite as the weight matrix, $\mathbf{M}$.

The energy norm for q can be rewritten as

$$\|q\|_E = \|\mathbf{F}q\|_2 = \|Fk\|_2 \qquad (2.19)$$

and the transient growth function (2.9) become

$$G(t) = \max \frac{\|q\|_E}{\|q_0\|_E} = \max \frac{\|\mathbf{F}q\|_2}{\|\mathbf{F}q_0\|_2} = \max \frac{\|Fk\|_2}{\|Fk_0\|_2} = \max \|F \, e^{\Lambda t} \, F^{-1}\|_2 \qquad (2.20)$$

In other words it is possibile to obtain the energy norm of q *measuring* it in the eigenvector space.

The main advantage of using equation (2.20) is that one computes the exponential of a diagonal matrix, i.e. Λt. Moreover it is possible to choose only a subset of the eigenvector, say the N eigenvectors related to the N more critical eigenvalues, e. g. for the Newtonian Hagen-Poiseuille flow the non normality of the differential operator relies in the eigenvectors related to the eigenvalues near the intersection of the branches of the characteristic Y-shaped spectrum.[10]

IN THE CASE OF FILTER MATRICES is it possible to use the projection onto the eigenvectors basis of the the energy norms defined with

[10] P. J. Schmid and D. S. Henningson (1994). "Optimal energy density growth in Hagen-Poiseuille flow". In: *J. Fluid Mech.* 277, pp. 197–225.

equations (2.12) and (2.13). For example considering q_{in}

$$E_{\text{in}} = \int_V q_{\text{in}}^{\text{T}} \mathbf{M}_{\text{in}} q_{\text{in}} \mathrm{d}V = \int_V q_0^{\text{T}} \mathbf{B}^{\text{T}} \mathbf{M}_{\text{in}} \mathbf{B} q_0 \mathrm{d}V$$
$$= \int_V k_0^{\text{T}} \ \mathbf{S}^{\text{T}} \mathbf{B}^{\text{T}} \mathbf{M}_{\text{in}} \mathbf{B} \mathbf{S} \ k_0 \mathrm{d}V \tag{2.21}$$

it is possible to obtain the matrix

$$M_{\text{in}} = \int_\Omega \mathbf{S}^{\text{T}} \mathbf{B}^{\text{T}} \mathbf{M}_{\text{in}} \mathbf{B} \mathbf{S} \ \mathrm{d}V \tag{2.22}$$

and its decomposition $M_{\text{in}} = F_{\text{in}}^{\text{T}} F_{\text{in}}$. Analogously it is possible to write $M_{\text{out}} = F_{\text{out}}^{\text{T}} F_{\text{out}}$ thus the transient growth becomes

$$G(t) = \max \frac{\|q_{\text{out}}\|_{E_{\text{out}}}}{\|q_{\text{in}}\|_{E_{\text{in}}}} = \max \frac{\|\mathbf{F}_{\text{out}} q_{\text{out}}\|_2}{\|\mathbf{F}_{\text{in}} q_{\text{in}}\|_2} = \max \frac{\|\mathbf{F}_{\text{out}} k\|_2}{\|\mathbf{F}_{\text{in}} k_0\|_2} \tag{2.23}$$

Remembering that

$$q = \mathbf{S} k = e^{\mathbf{L}t} \mathbf{B}^{\text{T}} q_{\text{in}} \tag{2.24}$$

where $q_{\text{in}} = \mathbf{B} q_0 = \mathbf{B} \mathbf{S} k_0$ ed $e^{\mathbf{L}t} = \mathbf{S} \ e^{\Lambda t} \mathbf{S}^{-1}$ it is possible to write

$$k = e^{\Lambda t} \mathbf{S}^{-1} \mathbf{B}^{\text{T}} \mathbf{B} \mathbf{S} k_0 \tag{2.25}$$

that give the correct projection of equation (2.20) onto the eigenvector space

$$G(t) = \max \|F_{\text{out}} e^{\Lambda t} \ \mathbf{S}^{-1} \mathbf{B}^{\text{T}} \mathbf{B} \mathbf{S} \ F_{\text{in}}^{-1}\|_2 \tag{2.26}$$

This equation is here proposed for the first time and even with some limitations that will be shown in the next chapters it will be an useful tool for inspecting the eigenspectrum of the linear differential operator involved in this work and its non-normal characteristics.

k_0 is the projection onto eigenvector basis of the generic initial vector of state q_0. This vector will have the zero components only *after* the filtering then.

$$k_0 = \mathbf{S}^{-1} q_0 \neq \mathbf{S}^{-1} q_{0\text{in}} = k_{\text{in}}$$

because

$$q_0 \neq q_{0\text{in}} = \mathbf{B}^{\text{T}} q_{\text{in}} = \mathbf{B}^{\text{T}} \mathbf{B} q_0$$

In particular it is true that

$$k_{\text{in}} = \mathbf{S}^{-1} \mathbf{B}^{\text{T}} \mathbf{B} \mathbf{S} k_0$$

3

PROBLEM FORMULATION

Linear stability analysis is performed on shear flows confined in a circular pipe, Hagen-Poiseuille flow (HPF), or between two coaxial circular cylinders, annular Poiseuille flow (APF). A cylindrical polar system of coordinates (r, θ, z) representing the radial, azimuthal and streamwise direction is considered in both cases and the corresponding velocity components are U, V and W.

THE STEADY SOLUTIONS for the Newtonian case are solution also for the flows of Oldroyd-B fluids, thus for the chosen geometries they are parallel flows of the type $\overline{U} = \{0, 0, \overline{W}(r)\}$. The dimensionless stationary solution for the Hagen-Poiseuille Flow is

$$\overline{W}(r) = 1 - r^2 \tag{3.1}$$

where the dimensionless radius r is obtained using as reference length the radius of the pipe $l = R$. For the annular Poiseuille flow the dimensionless solution is

$$\overline{W}(r) = \frac{r^2 + \frac{r_2^2 - r_1^2}{\log\left(\frac{r_2}{r_1}\right)} \log\left(\frac{r_2}{r}\right) - r_2^2}{\frac{r_2^2 - r_1^2}{\log\left(\frac{r_2}{r_1}\right)} \left[\frac{1}{2} + \log\left(\frac{r_2}{r_{\max}}\right)\right] - r_2^2} \tag{3.2}$$

where the reference length is $l = \frac{R_2 - R_1}{2}$, i.e. half of the gap between the inner cylinder with radius R_1 and the outer cylinder of radius R_2.

$r - \theta$ plane

r

■ R radius of the cylinder

REFERENCE Length: $l = R$

θ

PIPE Poiseuille flow

r

$r - z$ plane

z
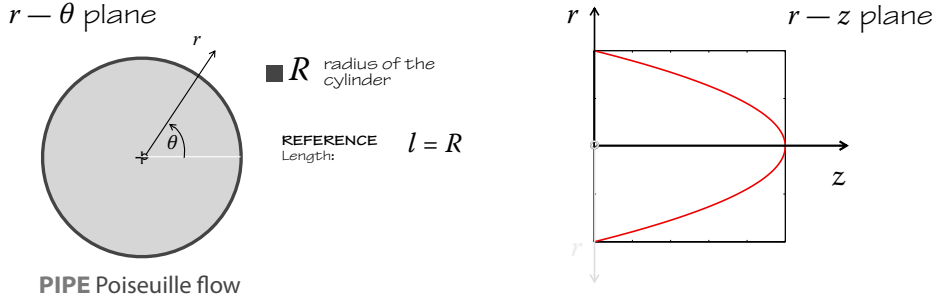
Figure 3.1: Hagen-Poiseuille Flow – base flow and geometry

The maximum velocity $\mathcal{U}$ has been taken as reference in both cases. For the Hagen-Poiseuille flow it is located on the symmetry axis, $r_{max} = 0$, while for the annular Poiseuille flow its location is given by

$$r_{max} = \sqrt{\frac{r_2^2 - r_1^2}{2\log\left(\frac{r_2}{r_1}\right)}}. \tag{3.3}$$

The annular geometry is interesting because can be interpreted as an intermediate configuration between the channel flow and the Hagen-Poiseuille flow. Introducing the *radii ratio* $\eta = r_1/r_2$ for η that tends to 1 the channel flow case is obtained while nullifying η the flow tends to the Hagen-Poiseuille flow.[1] An explicit expression of the conformation tensor corresponding to these base flows can be easily derived by equation (1.31) and written as

[1] C. J. Heaton (2008). "Linear instability of annular Poiseuille flow". In: *Journal of Fluid Mechanics* 610, pp. 391–406.

$$\overline{\mathsf{C}} = \begin{bmatrix} 1 & 0 & \mathcal{W}i\,\overline{W'} \\ & 1 & 0 \\ \mathrm{Sym} & & 1 + 2\mathcal{W}i^2\,\overline{W'}^2 \end{bmatrix} \tag{3.4}$$

where the symbol " $'$ " denotes derivation of the steady state quantities for r.

The base flow is perturbed so that the total velocity components pressure and conformation tensor become

$$\boldsymbol{U} = \overline{\boldsymbol{U}} + \boldsymbol{u}, \ P = \overline{P} + p, \ \mathsf{C} = \overline{\mathsf{C}} + \mathsf{c} \tag{3.5}$$

where capital letters mean (total) perturbed quantities, small letters infinitesimal disturbances and bar refers to the base flow.

$r - \theta$ plane

$r - z$ plane

ANNULAR Poiseuille flow

R_2 radius of the outer cylinder

R_1 radius of the inner cylinder

REFERENCE Length: $l = (R_2 - R_1)/2$

RADII Ratio: $\eta = R_1/R_2$

Figure 3.2: Annular Poiseuille Flow – base flow and geometry

Linearization is applied both to the Navier–Stokes equations

$$\nabla \boldsymbol{u} = 0 \tag{3.6}$$

$$\frac{\partial \boldsymbol{u}}{\partial t} + \overline{\boldsymbol{U}} \cdot \nabla \boldsymbol{u} + \boldsymbol{u} \cdot \nabla \overline{\boldsymbol{U}} = -\nabla p + \frac{\beta}{\mathcal{R}e} \nabla^2 \boldsymbol{u} + \frac{1-\beta}{\mathcal{R}e\,\mathcal{W}i} \nabla \cdot \mathbf{c} \tag{3.7}$$

and to the evolution equation for the polymer conformation tensor

$$\frac{\partial \mathbf{c}}{\partial t} + \boldsymbol{u} \cdot \nabla \overline{\mathbf{C}} + \overline{\boldsymbol{U}} \cdot \nabla \mathbf{c} - \mathbf{c} \cdot \nabla \overline{\boldsymbol{U}} - \overline{\mathbf{C}} \cdot \nabla \boldsymbol{u} - (\nabla \overline{\boldsymbol{U}})^{\mathrm{T}} \cdot \mathbf{c} - (\nabla \boldsymbol{u})^{\mathrm{T}} \cdot \overline{\mathbf{C}} = -\frac{\mathbf{c}}{\mathcal{W}i}. \tag{3.8}$$

Fourier decomposition in azimuthal and axial directions leads to the following expressions for disturbance quantities

$$[u, v, w, p](r, \theta, z, t) = [\hat{u}, \hat{v}, \hat{w}, \hat{p}](r, t) \cdot e^{i(m\theta + kz)} \tag{3.9}$$

$$[c_{rr}, c_{r\theta}, c_{rz}, c_{\theta\theta}, c_{\theta z}, c_{zz}](r, \theta, z, t) = [\hat{c}_{rr}, \hat{c}_{r\theta}, \hat{c}_{rz}, \hat{c}_{\theta\theta}, \hat{c}_{\theta z}, \hat{c}_{zz}](r, t) \cdot e^{i(m\theta + kz)} \tag{3.10}$$

where $m \in \mathbb{Z}$ and $k \in \mathbb{R}$ are the azimuthal and the axial wave numbers. Adding the temporal normal mode position leads to

$$[u, v, w, p](r, \theta, z, t) = [\tilde{u}, \tilde{v}, \tilde{w}, \tilde{p}](r) \cdot e^{i(m\theta + kz - \omega t)} \tag{3.11}$$

$$[c_{rr}, c_{r\theta}, c_{rz}, c_{\theta\theta}, c_{\theta z}, c_{zz}](r, \theta, z, t) = [\tilde{c}_{rr}, \tilde{c}_{r\theta}, \tilde{c}_{rz}, \tilde{c}_{\theta\theta}, \tilde{c}_{\theta z}, \tilde{c}_{zz}](r) \cdot e^{i(m\theta + kz - \omega t)} \tag{3.12}$$

where $\omega \in \mathbb{C}$ represents the temporal frequency. The real and imaginary parts of ω are respectively ω_r and ω_i and the amplitude functions (eigenfunctions) are denoted by the symbol "$\sim$". The projection

of (3.6), (3.7) and (3.8) to the chosen system of reference leads to equations reported on Appendix A.

The linearized equations can be reorganized in the following generalized eigenvalue problem

$$-i\omega \mathbf{N}\tilde{q} = \mathbf{A}\tilde{q} \qquad (3.13)$$

where $\tilde{q}$ is the phase space vector and contains the velocity components, conformation stress components and pressure. $\mathbf{N}$ is the unsteady operator and $\mathbf{A}$ is the convection-diffusion operator.

The problem is closed by specifying boundary conditions; for annular Poiseuille flow the velocity has to satisfy the homogeneous boundary conditions on the cylinders walls, for the Hagen-Poiseuille flow regularity conditions at $r = 0$ have to be specified for the velocity field in order to be continuous and single-valued.[2]

Regularity conditions at $r = 0$ have been derived for the conformation tensor too by imposing

$$\frac{\partial \mathbf{c}}{\partial \theta} = 0 \qquad (3.14)$$

that, taking into account equation (3.12), leads to

$$im \begin{bmatrix} \tilde{c}_{rr} & \tilde{c}_{r\theta} & \tilde{c}_{rz} \\ & \tilde{c}_{\theta\theta} & \tilde{c}_{\theta z} \\ \mathrm{Sym} & & \tilde{c}_{zz} \end{bmatrix} + \begin{bmatrix} -2\tilde{c}_{r\theta} & \tilde{c}_{rr} - \tilde{c}_{\theta\theta} & -\tilde{c}_{\theta z} \\ & 2\tilde{c}_{r\theta} & \tilde{c}_{rz} \\ \mathrm{Sym} & & 0 \end{bmatrix} = 0 \qquad (3.15)$$

that can be rewritten as

$$\begin{bmatrix} im & 0 & 0 & -2 & 0 & 0 \\ 0 & im & 0 & 2 & 0 & 0 \\ 0 & 0 & im & 0 & 0 & 0 \\ 1 & -1 & 0 & im & 0 & 0 \\ 0 & 0 & 0 & 0 & im & -1 \\ 0 & 0 & 0 & 0 & 1 & im \end{bmatrix} \begin{bmatrix} \tilde{c}_{rr} \\ \tilde{c}_{\theta\theta} \\ \tilde{c}_{zz} \\ \tilde{c}_{r\theta} \\ \tilde{c}_{rz} \\ \tilde{c}_{\theta z} \end{bmatrix} = 0 \qquad (3.16)$$

If the determinant of the matrix in equation (3.16) is not zero the only admissible solution is the homogeneous one and then the compatibility conditions on the axis are all zeros. This is the case of $m > 2$.

Otherwise the following conditions can be obtained

$m = 0$

$$\tilde{c}_{rr} - \tilde{c}_{\theta\theta} = \tilde{c}_{r\theta} = \tilde{c}_{rz} = \tilde{c}_{\theta z} = 0$$
$$\tilde{c}_{zz} \text{ finite} \qquad (3.17)$$

[2] M. R. Khorrami et al. (1989). "Application of spectral collocation techniques to the stability of swirling flows". In: *J. Comp. Phys.* 81, pp. 206–229; R. L. Ash and M. R. Khorrami (1995). "Vortex Stability in *Fluid Vortices*". In: Kluwer, pp. 317–372.

$m = \pm 1$

$$\tilde{c}_{rr} = \tilde{c}_{\theta\theta} = \tilde{c}_{zz} = \tilde{c}_{r\theta} = \tilde{c}_{rz} + i\tilde{c}_{\theta z} = 0 \tag{3.18}$$

$m = \pm 2$

$$\tilde{c}_{zz} = \tilde{c}_{rz} = \tilde{c}_{\theta z} = \tilde{c}_{rr} + \tilde{c}_{\theta\theta} = \tilde{c}_{rr} + i\tilde{c}_{r\theta} = 0 \tag{3.19}$$

The failure of the eigenvalue problem in predicting the experimental critical values of the parameters that trigger transitions in wall bounded flows is well known; thus more recent studies have pointed out the importance of the transient behavior of initial disturbances due to the non-normality of the evolution operator.

The problem is then cast in an initial value problem of the type

$$\frac{\partial \hat{\psi}}{\partial t} = \mathbf{L}\hat{\psi} \tag{3.20}$$

In order to obtain the differential operator $\mathbf{L}$ it has been necessary to recast the set of differential equations in a more compact form that eliminates the singularity in the differential operator $\mathbf{N}$ used in equation (3.13). Resolving the conservation of mass for w and the momentum balance along z for p and substituting in the other equations leads to the set of governing equation for the recast vector of state $\psi = [u, v, c_{rr}, c_{r\theta}, c_{rz}, c_{\theta\theta}, c_{\theta z}, c_{zz}]^{\mathrm{T}}$.

As written above, only the initial disturbances that have zero value for the conformation tensor components, i.e. $\psi_0 = [u, v, 0, 0, 0, 0, 0, 0]^{\mathrm{T}}$, are considered and only the kinetic energy of the evolved phase vector is monitored. This is made possible by defining the *filter* matrix

$$\mathbf{B} = \begin{bmatrix} 1 & 0 & 0 & 0 & 0 & 0 & 0 & 0 \\ 0 & 1 & 0 & 0 & 0 & 0 & 0 & 0 \end{bmatrix}$$

for both the output and input vectors so that $\psi_0 = \mathbf{B}^{\mathrm{T}}\psi_{\mathrm{in}}$ and $\psi_{\mathrm{out}} = \mathbf{B}\,\psi$. For the generic *filtered* vectors ψ_{f}, i.e. ψ_{in} and ψ_{out}, the kinetic energy is

$$E_{\mathrm{K}} = \frac{1}{2} \int_{\Omega} \psi_{\mathrm{f}}^* \, \mathbf{M} \, \psi_{\mathrm{f}} \; \mathrm{d}\Omega \tag{3.21}$$

where $\mathbf{M}$ is the energy weight matrix that can expressed as $\mathbf{M} = \mathbf{F}^{\mathrm{T}}\mathbf{F}$ with a Cholesky decomposition. Being $\mathbf{T} = \mathbf{B}\,e^{\mathbf{L}t}\,\mathbf{B}^{\mathrm{T}}$ the evolution tensor that routes from ψ_{in} to ψ_{out}, the growth function is

$$G(t) = \max \frac{\|\psi_{\mathrm{out}}\|_{E_{\mathrm{out}}}}{\|\psi_{\mathrm{in}}\|_{E_{\mathrm{in}}}} = \|\mathbf{F}\mathbf{B}\,e^{\mathbf{L}t}\,\mathbf{B}^{\mathrm{T}}\mathbf{F}^{-1}\|_2 \tag{3.22}$$

Kinetic Energy Budget

An useful tool for gaining a deeper understatement of the mechanism that leads to instabilities is the kinetic energy analysis. By multiplying the linearized momentum equations written for the generic Fourier mode by the complex conjugates of $\hat{u}$, $\hat{v}$, $\hat{w}$, and subsequently integrating over the domain the following expression of the kinetic energy budget can be obtained

$$
\begin{aligned}
\frac{1}{2}\frac{\partial}{\partial t}\int_{\Omega}\|\boldsymbol{u}\|^2 r\,\mathrm{d}r = & -\operatorname{Re}\left\{\int_{\Omega}\left(\overline{W'}\hat{u}\hat{w}^*\right)r\,\mathrm{d}r\right\} - \hat{u}^*\hat{p}r\Big|_{B\Omega} + \frac{\beta}{\mathcal{R}e}\left[\hat{u}^*\frac{\partial(\hat{u}r)}{\partial r}\Big|_{B\Omega} + \hat{v}^*\frac{\partial(\hat{v}r)}{\partial r}\Big|_{B\Omega} + \hat{w}^*r\frac{\partial\hat{w}}{\partial r}\Big|_{B\Omega}\right] & + \\
& -\frac{\beta}{\mathcal{R}e}\int_{\Omega}\left[\frac{1}{r^2}\Big|\frac{\partial(\hat{u}r)}{\partial r}\Big|^2 + \frac{1}{r^2}\Big|\frac{\partial(\hat{v}r)}{\partial r}\Big|^2 + \Big|\frac{\partial\hat{w}}{\partial r}\Big|^2 + \frac{4m}{r^2}\operatorname{Im}\{\hat{u}\hat{v}^*\} + \left(\frac{m^2}{r^2}+k^2\right)\|\boldsymbol{u}\|^2\right]r\,\mathrm{d}r & + \\
& +\operatorname{Re}\left\{\frac{1-\beta}{\mathcal{W}i\mathcal{R}e}\int_{\Omega}\left[\left(\frac{\hat{c}_{rr}}{r} + \frac{\partial\hat{c}_{rr}}{\partial r} + \frac{im}{r}\hat{c}_{r\theta} + ik\hat{c}_{rz} - \frac{\hat{c}_{\theta\theta}}{r}\right)\hat{u}^*\right.& + \\
& \left.+\left(\frac{2\hat{c}_{r\theta}}{r} + \frac{\partial\hat{c}_{r\theta}}{\partial r} + \frac{im}{r}\hat{c}_{\theta\theta} + ik\hat{c}_{\theta z}\right)\hat{v}^* + \left(\frac{\hat{c}_{rz}}{r} + \frac{\partial\hat{c}_{rz}}{\partial r} + \frac{im}{r}\hat{c}_{z\theta} + ik\hat{c}_{zz}\right)\hat{w}^*\right]r\,\mathrm{d}r\right\}
\end{aligned}
$$
$$(3.23)$$

where $\|\boldsymbol{u}\|^2 = (|\hat{u}|^2 + |\hat{v}|^2 + |\hat{w}|^2)$, Ω is the domain of integration and $B\Omega$ its boundary. The following terms can be recognized in equation 3.23

$$\dot{E}_{\mathrm{K}} = \frac{\partial E_{\mathrm{K}}}{\partial t} = \frac{1}{2}\frac{\partial}{\partial t}\int_{\Omega}\|\hat{\boldsymbol{u}}\|^2 r\,\mathrm{d}r$$

$$I = -\operatorname{Re}\left\{\int_{\Omega}\left(\overline{W'}\hat{u}\hat{w}^*\right)r\,\mathrm{d}r\right\}$$

$$D_{\mathrm{v}} = -\frac{\beta}{\mathcal{R}e}\int_{\Omega}\left[\frac{1}{r^2}\Big|\frac{\partial(\hat{u}r)}{\partial r}\Big|^2 + \frac{1}{r^2}\Big|\frac{\partial(\hat{v}r)}{\partial r}\Big|^2 + \Big|\frac{\partial\hat{w}}{\partial r}\Big|^2 + \frac{4m}{r^2}\operatorname{Im}\{\hat{u}\hat{v}^*\} + \left(\frac{m^2}{r^2}+k^2\right)\|\boldsymbol{u}\|^2\right]r\,\mathrm{d}r$$

$$W_{\mathrm{p}} = +\operatorname{Re}\left\{\frac{1-\beta}{\mathcal{W}i\mathcal{R}e}\int_{\Omega}\left[\left(\frac{\hat{c}_{rr}}{r} + \frac{\partial\hat{c}_{rr}}{\partial r} + \frac{im}{r}\hat{c}_{r\theta} + ik\hat{c}_{rz} - \frac{\hat{c}_{\theta\theta}}{r}\right)\hat{u}^* + \right.$$
$$\left. +\left(\frac{2\hat{c}_{r\theta}}{r} + \frac{\partial\hat{c}_{r\theta}}{\partial r} + \frac{im}{r}\hat{c}_{\theta\theta} + ik\hat{c}_{\theta z}\right)\hat{v}^* + \left(\frac{\hat{c}_{rz}}{r} + \frac{\partial\hat{c}_{rz}}{\partial r} + \frac{im}{r}\hat{c}_{z\theta} + ik\hat{c}_{zz}\right)\hat{w}^*\right]r\,\mathrm{d}r\right\}$$

where $\dot{E}_{\mathrm{K}}$ is the kinetic energy rate, I the Reynolds stress production , D_{v} viscous dissipation and W_{p} is the rate of work done by the polymer on the flow, it is an exchange term and its sign is indefinite. The boundary condition contribution to the kinetic energy budget is

$$B = -\frac{\beta}{\mathcal{R}e}\left[|\hat{u}(0)|^2 + |\hat{v}(0)|^2\right]; \qquad (3.24)$$

and equation 3.23 can be written arranged as

$$\dot{E}_{\mathrm{K}} = I + D_{\mathrm{v}} + W_{\mathrm{p}} + B \qquad (3.25)$$

For the APF the boundary contribution B is zero because of the homogeneous conditions thus

$$\dot{E}_K = I + D_v + W_p \qquad (3.26)$$

CODE DESCRIPTION AND VALIDATION

The generalized eigenvalue problem (3.13) has been discretized along the radial direction by employing a standard Chebyshev collocation method; the finite domain has been mapped to the interval $[-1, 1]$ via a linear transformation. Boundary conditions on the walls and/or on the axis are enforced by replacing rows.

Moreover a particular attention has been given to the boundary conditions of the initial value problem expressed by equation (3.20) in order to avoid unphysical spurious eigenvalues. These highly unstable eigenvalues, that drastically affect the behaviour of the linear operator, are different from numerical spurious ones and occur mainly because of misapplications (e.g. redundancies) of the boundary conditions.[3]

Validation

The narrow gap limit of the annular flow is the planar Poiseuille flow. This fact has been useful during the code validation phase. The results obtained for the annular configuration for r_1 tending to infinity, i.e. η tending to 1, have been validated against the references found in literature for the channel flow of viscoelastic fluids.[4]

The convergence for increasing r_1 of the least stable eigenvalue, ω_{cr}, to the values provided by Sureshkumar and Beris for the flow parameters $\mathcal{R}e = 3960, \beta = 0.5, \mathcal{W}i = 3.96, k = 1.15$ and $m = 0$ has been verified using a grid of 129 points. The results are plotted in Figure 3.4. Numerical values for r_1 equal to 10^2, 10^3 and 10^4 are reported in Table 3.1 and compared to the ones found in works by Sureshkumar and Beris and Zhang et al.

In Figure 3.3 the complete eigenspectrum obtained for $r_1 = 10^3$, $\mathcal{R}e = 2310, \mathcal{W}i = 2.31, \beta = 0.5, k = 1.31, m = 0$ and two values of the grid points numbers, $N = 128$ and $N = 256$, is plotted. It has been compared to the results presented by Sureshkumar and Beris for the same flow parameters and the same numbers of grid points and and an complete agreement with eigenvalues depicted in black has been found

[3] J. P. Boyd (2000). *Chebyshev and Fourier spectral methods*. Second Edition. Dover Publications.

[4] R. Sureshkumar and A. N. Beris (1995). "Linear stability analysis of channel flow of viscoelastic Oldroyd-B and FENE-P fluids". In: *Journal of Non-Newtonian Fluid Mechanics* 56, pp. 151–182; Zhang et al., "Linear stability analysis of channel flow of viscoelastic Oldroyd-B and FENE-P fluids".

ANNULAR FLOW		CHANNEL FLOW	
r_1	ω_{cr}		ω_{cr}
10^2	$0.34088888 - 1.0122 \times 10^{-5}\mathrm{i}$	SB	$0.34089442 + 1.9696 \times 10^{-7}\mathrm{i}$
10^3	$0.34089435 + 0.9379 \times 10^{-7}\mathrm{i}$	Zhang et al.	$0.34089441 + 1.9888 \times 10^{-7}\mathrm{i}$
10^4	$0.34089441 + 1.9875 \times 10^{-7}\mathrm{i}$		

Table 3.1: Validation of the code for the annular pipe flow against the results by Sureshkumar & Beris and Zhang *et al.* for channel flow of an Oldroyd–B fluid

for both $N = 128$ and $N = 256$. These are the eigenvalues related to the non-swirling components of the velocity, u and w, that are decoupled from the component in the azimuthal direction, v.

Because of the Squire's theorem that has been proven valid also for Oldoryd-B fluids, Sureshkumar and Beris consider only two-dimensional disturbances and this is why the eigenvalues related to the azimuthal direction (depicted in red) do not appear in their analysis.

Indeed for $m = 0$ equations (A.1), (A.2), (A.4), (A.5), (A.8), (A.10) and (A.7) related to the components $\{u, w, c_{rr}, c_{\theta\theta}, c_{zz}, c_{rz}\}$ of the state vector are decoupled from equations (A.3), (A.6), (A.9) related to $\{v, c_{r\theta}, c_{\theta z}\}$ and the complete eigenspectrum can be obtained as superposition of two distinct eigenspectra.

for these equations see Appendix A
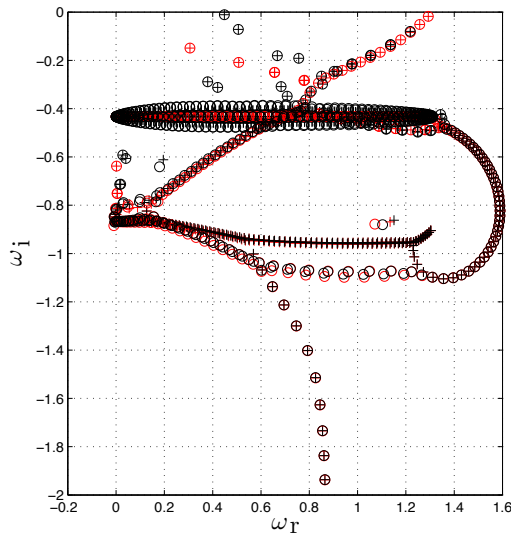
Figure 3.3: $\mathcal{R}e = 2310$, $\mathcal{W}i = 2.31$, $\beta = 0.5$, $k = 1.31$, $m = 0$, $r_1 = 10^3$, $N = 128(\circ)$ & $N = 256(+)$
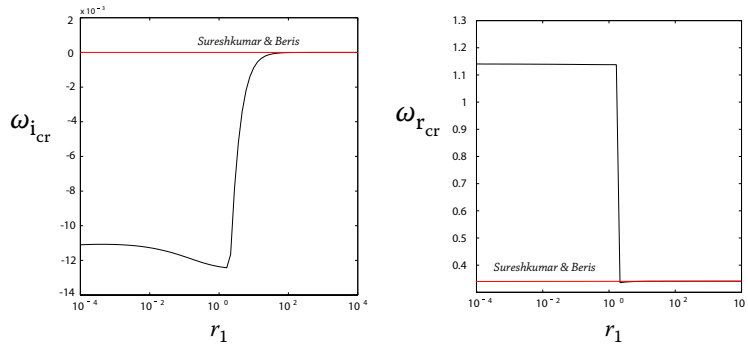
Figure 3.4: Least stable eigenvalue for varying r_1. $Re = 3960$, $\beta = 0.5$, $Wi = 3.96$, $k = 1.15$ and $m = 0$

While the Squire's theorem for the planar flow allows to consider only the longitudinal disturbances for the linear stability analysis of both Newtonian and Oldroyd-B fluids, for the cylindrical case also the swirling disturbances must be taken into account because there is no analogue of such a theorem for this configuration.[5]

This is confirmed by preliminary tests on the least stable eigenvalue ω_{cr} of the APF for $m = 0$ conducted by varying the inner radius r_1. The results for the case of $Re = 3960$, $\beta = 0.5$, $Wi = 3.96$, $k = 1.15$ are plotted in Figure 3.4. In Figure 3.4 a discontinuity in the first derivative of $\omega_{i_{cr}}$ can be seen for $r_1 \approx 10^{0.317}$; for the same value of r_1 a discontinuity in $\omega_{r_{cr}}$ occurs too. These discontinuities are due to the fact that for great values of the inner radius the leading eigenvalue belongs to the part of the spectrum of the longitudinal disturbances, as it has to be for the Squire's theorem, while for small values it belongs to the one related to the azimuthal disturbances. A further confirmation is given by the eigenspectra calculated for $r_1 = 1$ and $r_1 = 10$ that are plotted in Figures 3.5 and 3.6 respectively alongside the eigenfunctions related to the least stable eigenvalue, ω_{cr}.

Zhang performed the modal energy analysis on the channel flow of a FENE-P fluid. The limit of the of the FENE–P constitutive equation for the maximum extensibility of the polymer L tending to infinity is the Oldroyd–B model. A comparison between the results of the modal energy analysis performed on the channel flow of a FENE-P fluid for $Re = 5600$, $Wi = 6$, $\beta = 0.9$, $k = 1.02$, $m = 0$, $L = 500$ and the results obtained for the narrow gap limit, $r_1 = 10^3$, of the annular pipe flow
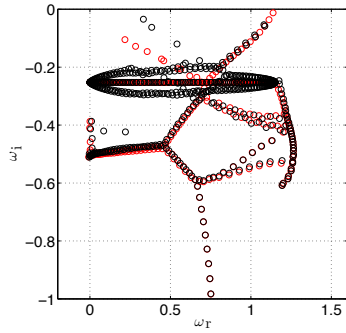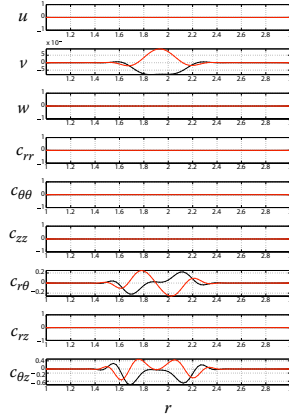
(a) Eigenspectrum

(b) Eigenfunctions for ω_{cr}

Figure 3.5: $\mathcal{R}e = 3960$, $\beta = 0.5$, $\mathcal{W}i = 3.96$, $k = 1.15$, $m = 0$, $r_1 = 1$: a) Planar ($\circ$) and azimuthal ($\circ$) parts of the eigenspecrtum; b) real ($-$) and imaginary ($-$) parts of the eigenfunctions for $\omega_{cr} = 1.137808371378438 - 0.012362801674458i$ (b)
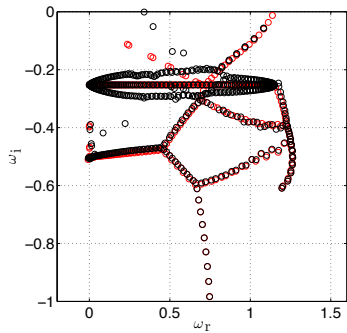
(a) Eigenspectrum
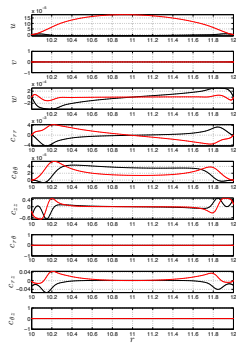
(b) Eigenfunctions for ω_{cr}

Figure 3.6: $\mathcal{R}e = 3960$, $\beta = 0.5$, $\mathcal{W}i = 3.96$, $k = 1.15$, $m = 0$, $r_1 = 10$: a) Planar ($\circ$) and azimuthal ($\circ$) parts of the eigenspecrtum; b) real ($-$) and imaginary ($-$) parts of the eigenfunctions for $\omega_{cr} = 0.340432582595774 - 0.000876450762291i$ (b)

Terms	APF Oldroyd–B	Zhang *et alii*
D_v	-14.456 $\times 10^{-4}$	-14.449 $\times 10^{-4}$
W_p	-137.533 $\times 10^{-4}$	-137.530 $\times 10^{-4}$
I	150.151 $\times 10^{-4}$	149.969 $\times 10^{-4}$
TOTAL	-1.838 $\times 10^{-4}$	-2.010 $\times 10^{-4}$
$2\omega_\mathrm{i}$	-1.838 $\times 10^{-4}$	-2.010 $\times 10^{-4}$

Table 3.2: Comparison between modal energy analysis of the annular pipe flow of an Oldroyd–B fluid for $r_1 = 10^3$, $\mathcal{R}e = 5600$, $\mathcal{W}i = 6$, $\beta = 0.9$, $k = 1.02$, $m = 0$ and the results by Zhang et al. for the channel flow of a FENE–P fluid with $L = 500$

of an Oldroyd-B fluid with same parameters is shown in Table 3.2. The imaginary part of ω_cr for the Oldroyd-B costitutive equation is greater than for the FENE model, confirming the stabilizing effect of the finite extensibility of the polymeric chains. The main cause of this behaviour seem rely mainly in a greater Reynolds stress production I; sinstead the polymeric and viscous dissipation D_v and W_p are almost the same for both case.

Larson in 1992 stated the lack of works dealing with the linear stability of viscoelastic inertial flows past circular pipes and even if nowadays some weakly non-linear analysis on the inertialess Hagen-Poiseuille flow of viscoelastic fluids have been found,[6] the linear stability of the inertial regime of Oldroyd-B fluids in circular pipes has not been investigated yet, thus only the Newtonian case has been used as reference.[7]

As it has been seen the Newtonian limit can be reached starting by the Oldroyd-B in two ways, i.e for $\beta = 1$ or for $\mathcal{W}i \to 0$. While the former leads to the trivial decoupling of equation (1.31) and (1.31), the limit for $\mathcal{W}i \to 0$ is much more interesting. In this case the two equations remains coupled while the stress tensor related to the polymer contribution must act as the viscous dissipation.

Converge tests has been performed for the Hagen-Poiseuille flow for the Weissenberg number, $\mathcal{W}i$, tend to zero. In Figure 3.7 it is highlighted both the imaginary part of the least stable eigenvalue and the complete eigenspectrum converge to the values of the Newtonian case.

Even if the transient growths presented in Chapter 4 have been computed using equation (3.22), some tests have been made with equation (2.26) proposed in 2 that uses the projection onto the eigenvectors basis.

As it happens for the Newtonian case of the circular pipe flow[8] the

[6] B. Meulenbroek et al. (2004). "Weakly nonlinear subcritical instability of visco-elastic Poiseuille flow". In: *Journal of Non-Newtonian Fluid Mechanics* 116, pp. 235–268.

[7] see Schmid and Henningson, "Optimal energy density growth in Hagen-Poiseuille flow".

[8] Schmid and Henningson, "Optimal energy density growth in Hagen-Poiseuille flow".

eigenspectrum

imaginary part of the least stable eigenvalue
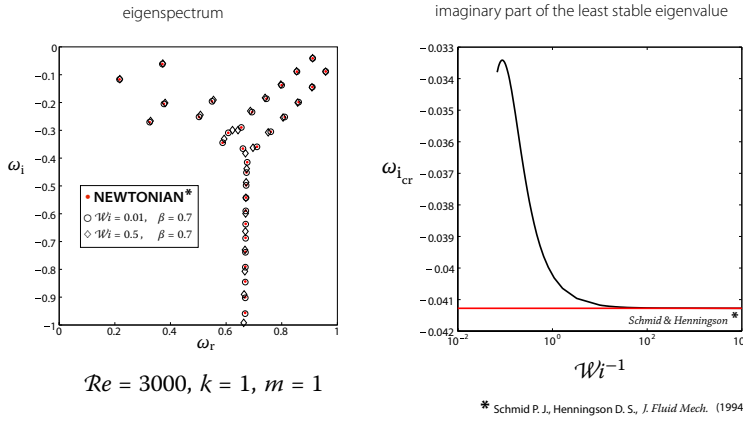
$\mathcal{R}e = 3000, k = 1, m = 1$

Figure 3.7: Validation of the eigenspectrum of the Hagen-Poiseuille flow of an Oldoryd-B fluid against the Newtonian case (Schmid and Henningson) $\mathcal{R}e = 3000, k = 1, m = 1, \beta = 0.7$ at various $\mathcal{W}i$

* Schmid P. J., Henningson D. S., *J. Fluid Mech.* (1994)

convergence of the growth function can be gained by using only few eigenvectors. Convergence to the reference growth function computed by the mean of equation (3.22) for parameters $\mathcal{R}e = 1000, \beta = 0.45, \mathcal{W}i = 1, k = 0.5, m = 0, \eta = 0.5$ are presented in Figure 3.8. Using just the first $N_{\text{eig}} = 21$ eigenvectors, i.e. the eigenvectors with $\omega_{\text{i}} > -0.5$, suffice to obtain the 98 % of the total G_{max}.

From a computational point of view this seems to be advantageous because the matrix involved for computing the reference value (black line) with equation (3.22) is of dimensions $6N \times 6N$; moreover bad calculated eigenvectors[9] are not included in the computation. However equation (2.26) gives some problems at the time step $t = 0$ where the value of $G(t) \neq 1$, that seems to be related to the unsuitableness of such a few eigenvectors to describe the constraint of zero values for the conformation tensor components.

[9] i.e. the numerical spurious eigenvalues

Spectrum structure

The spectrum structure of the Hagen-Poiseuille flow of an Oldoryd-B fluid is quite easily recognizable from previous observations on the spectrum of both inertialess and inertial case of the channel flow.[10] In Figure 3.9 the eigenspectra computed for two sets of governing parameters are plotted.

In this figure it is possible to individuate the characteristic Y-shaped part of the Newtonian case, a continuum spectrum located at $-1/\mathcal{W}i$

[10] see H. J. Wilson et al. (1999). "Structure of the spectrum in zero Reynolds number shear flow of the UCM and Oldroyd-B liquids". In: *Journal of Non-Newtonian Fluid Mechanics* 80.2, pp. 251–268; Sureshkumar and Beris, "Linear stability analysis of channel flow of viscoelastic Oldroyd-B and FENE-P fluids".
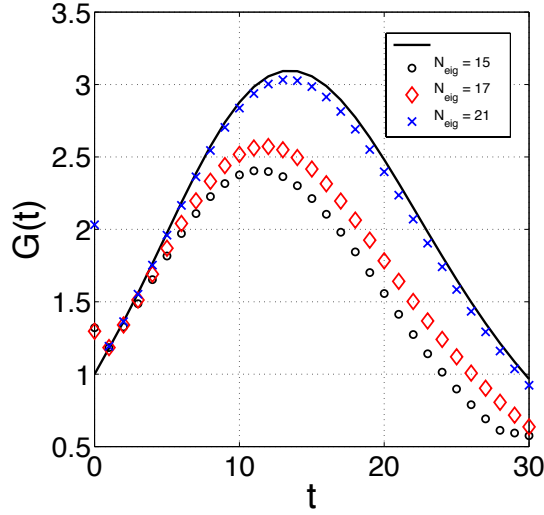
and a second continuum spectrum located at $-\frac{1}{\beta \cdot \mathcal{W}i}$. Moreover because of the smallness of the streamwise wave number, $k = 1$ in both sets of parameter, an almost circular structure can be seen. The center of this circle is approximately at $2/3k - \frac{1}{\beta \cdot \mathcal{W}i}$i and the mean radius is almost $|\frac{1}{\beta \cdot \mathcal{W}i} - \frac{1}{2\mathcal{W}i}|$, thus tends to infinity for the UCM case, $\beta \rightarrow 0$ and the circle tends to a line located at $-\frac{1}{2\mathcal{W}i}$ reported by Sureshkumar and Beris for the UCM fluid.

Increasing the value of k stretches this circle that firstly becomes elliptical and for further increments, i.e. when k becomes comparable to $\frac{1}{\beta \cdot \mathcal{W}i}$, the circle drastically changes and becomes a more complex structure (see Figure 3.3). The azimuthal wave number m does not affect this part of the spectrum.
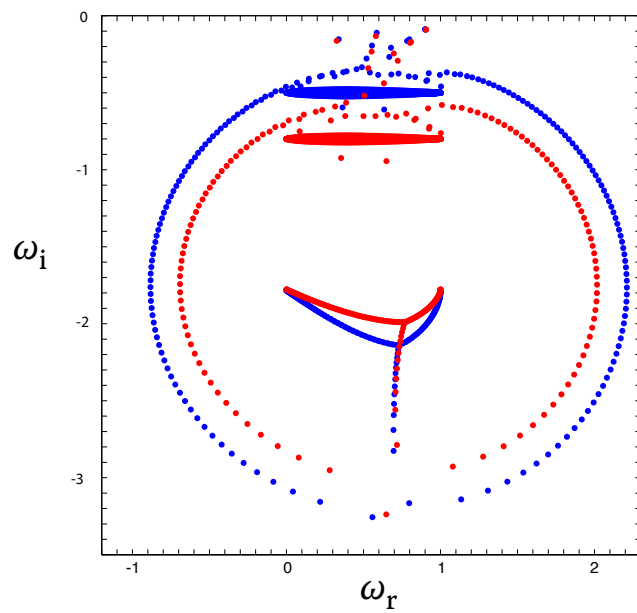
Figure 3.9: Spectrum structure for $k = 1$.
(•) $\mathcal{Re} = 1000$, $m = 0$, $\beta = 0.28$, $\mathcal{Wi} = 2$;
(•) $\mathcal{Re} = 1000$, $m = 0$, $\beta = 0.45$, $\mathcal{Wi} = 1.25$.

4

STABILITY ANALYSIS OF ANNULAR PIPE FLOW

The modal and non-modal linear stability of Oldroyd-B fluids in the annular pipe flow configuration is investigated in this chapter .

The choice of analyzing in detail such kind of flow is due to the large application of non-Newtonian flow in annular horizontal pipe in many industrial process, two example being annular heat exchangers in the food industry and drilling operations, and moreover because, as just told in Chapter 3, this geometry can be interpreted as an intermediate configuration between the channel flow and the Hagen-Poiseuille flow: for a radii ratio η tending to 0 the flow tends to the one in a circular pipe, while for a radii ratio tending to infinite the channel flow limit is reached. Here, indeed, parametric analysis, by varying the fundamental parameters governing the flow, in particular the radii ratio, η, the Weissenberg number $\mathcal{W}i$ and the viscosity ratio, β, are presented.

Among the first studies on the modal stability analysis of inertial flow of viscoelastic fluids the most relevant are by Porteous and Denn in 1972 and Ho and Denn in 1977, followed by Sureshkumar and Beris in 1995. A more extensive explanation of the non-monotonic viscoelastic effects on the critical Reynolds number is given by Sadanandan and Sureshkumar in 2002. All these works deals with the plane Poiseuille case.

The non-modal effects on the linear stability of viscoealstic fluids has been investigated by authors such as Hoda et al., Jovanović and Kumar and Zhang et al. only in recent times. All these authors have studied the energy amplification of Oldroyd-B fluids again only for

channel flow. Hoda et al., Jovanović and Kumar studied the transient growth of the instabilities from an *input-output* point of view, considering the amplification of stochastic disturbances, while Zhang et al. explained the energy amplification by a more classical initial value problem approach, even modified by the mean of the filter matrices.

The non-modal analysis has been here performed by using the *filter method* that has been extensively explained in Chapter 2 and just the kinetic energy of the flow has been considered. The effects of both two-dimensional and three-dimensional perturbations have been taken into account and comparisons with the Newtonian case, obtained as limit of the Oldroyd-B model for the viscosity ratio β tending to 1 or for the Weissenberg number $\mathcal{W}i$ tending to 0,[1] are reported in order to better understand the different behaviour of viscoelastic fluids.

[1] see Chapter 1 for further details.

MODAL STABILITY ANALYSIS

Neutral stability curves in the $(k, \mathcal{R}e)$ plane are the points defined by the couples of k and $\mathcal{R}e$ for which the imaginary part of the most critical eigenvalue, $\omega_{i_{cr}}$, obtained solving the eigenvalue problem expressed by equation (3.13) is zero. They can be seen as the delimitation between the zone of stable $(k, \mathcal{R}e)$, that is the area included in the curves, and the zone of parameters leading to modal instability.

Given a neutral curve there is a value of the Reynolds number for which only one disturbance, related to a particular value of the streamwise wavenumber k, is stable. This value of the $\mathcal{R}e$ is the *critical* Reynolds number, $\mathcal{R}e_{cr}$, and its associated wavenumber is k_{cr}.

Modifications of the neutral stability curves caused by the viscosity ratio, β, the Weissenberg number, $\mathcal{W}i$, and inner radius, r_1 have been evaluated.

In Figure 4.1 the effect of the viscosity ratio β on the marginal curves for two values of the inner radius, $r_1 \in \{2, 5\}$, and two values of the Weissenberg number, $\mathcal{W}i \in \{1, 15\}$ are presented. The macroscopic effect of decreasing the radii ratio η and then tending to the circular pipe is to increase the critical value of the Reynolds number, $\mathcal{R}e_{cr}$. Moreover for small values of $\mathcal{W}i$, i.e. $\mathcal{W}i \ll 10$, the effect of decreasing β is always destabilizing, while for greater values of the Weissenberg number the effect is slightly stabilizing before becoming destabilizing. This behaviour can be seen also in Figure 4.3.

$Wi = 1$ $Wi = 15$

$r_1 = 5$

$r_1 = 2$
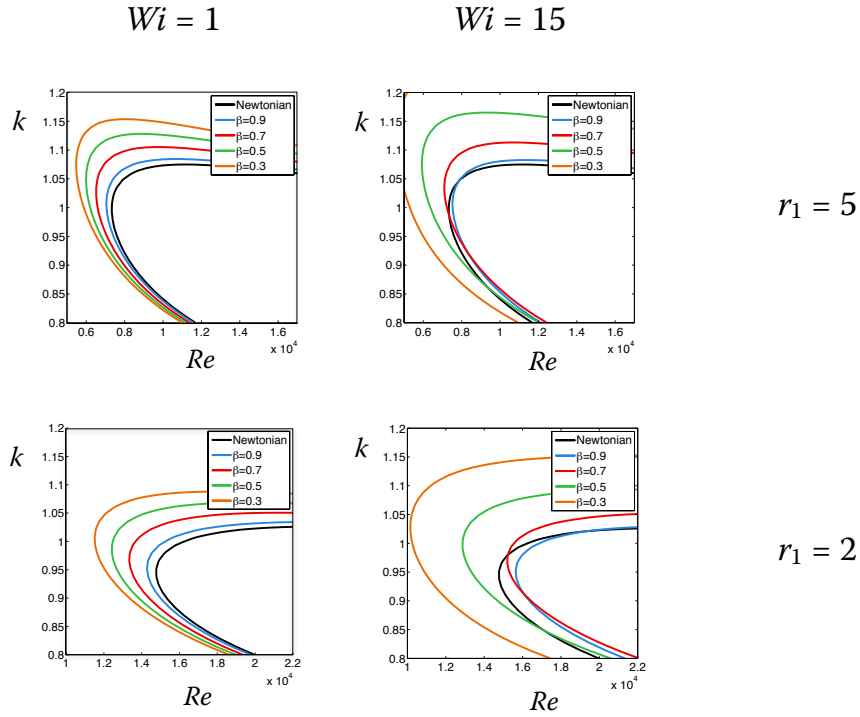
Figure 4.1: Modifications on the neutral curves depending on β. The effect of β is always destabilizing for small values of Wi.

In Figure 4.2 the effect of the Weissenberg number Wi on the marginal curves for two values of the inner radius, $r_1 \in \{2, 5\}$, and two values of the viscosity ratio, $\beta \in \{0.7, 0.9\}$ are presented. Starting from the Newtonian case (black line) the increase of the Weissenberg number has a mixed effect on the modal stability of the flow. At the beginning it destabilizes the flow and thus the Re_{cr} diminishes until a certain value of Wi is reached above which further increases of Wi become stabilizing. The range of Wi, in which the destabilization occurs, depends on the inner radius r_1; for the $r_1 = 5$ case there is destabilization for Wi up to approximately 2 while for $r_1 = 2$ the increase of the Weissenberg number is destabilizing for Wi up to 5. Hence when the geometry tends to the circular pipe an extension of the range of destabilizing Wi appears.

The non-monotonic dependence of the critical Reynolds number on Wi is highlighted in Figure 4.3 where the Re_{cr} is graphed as a function
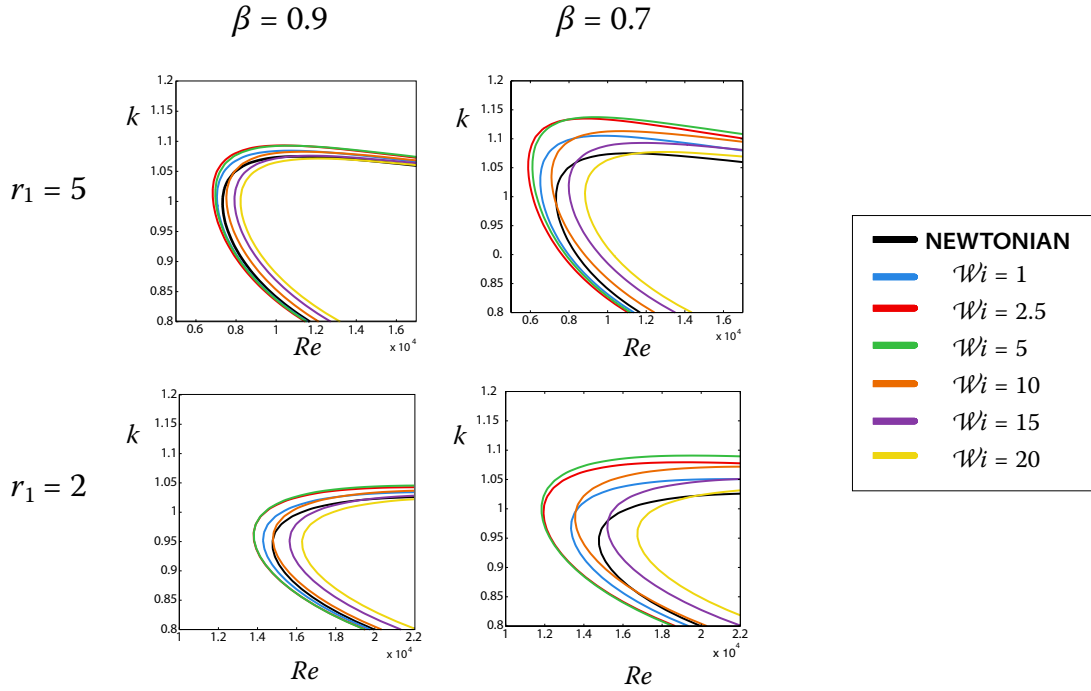
Figure 4.2: Neutral curves for varying $\mathcal{W}i$

of $\mathcal{W}i$ for $m = 0$. This behaviour is analogous to what happens in the channel flow case.[2] The results have been obtained for three different values of the viscosity ratio, $\beta = \{0.9, 0.7, 0.5\}$, and for two different values of the inner radius, $r_1 = \{5, 2\}$, computing the critical Reynolds number and its associated streamwise wavenumber k_{cr} that in general differs for each point.

The effects of the inner radius r_1 (or equivalently of the radii ratio of the annulus, η) can be better understood using the radius of the outer cylinder, i.e. the radius of the complete pipe, as the reference length and introducing the corresponding Reynolds number, $\mathcal{R}e\,r_2$. In Figure 4.4 the Weissenberg number $\mathcal{W}i$ is plotted as a function of $(\mathcal{R}e_{cr} - \mathcal{R}e_{cr\,|\,\text{Newt}})\,r_2$, i.e. the critical Reynolds number referred to r_2 and normalized with the critical Reynolds number of the Newtonian

[2] see Sureshkumar and Beris, "Linear stability analysis of channel flow of viscoelastic Oldroyd-B and FENE-P fluids".
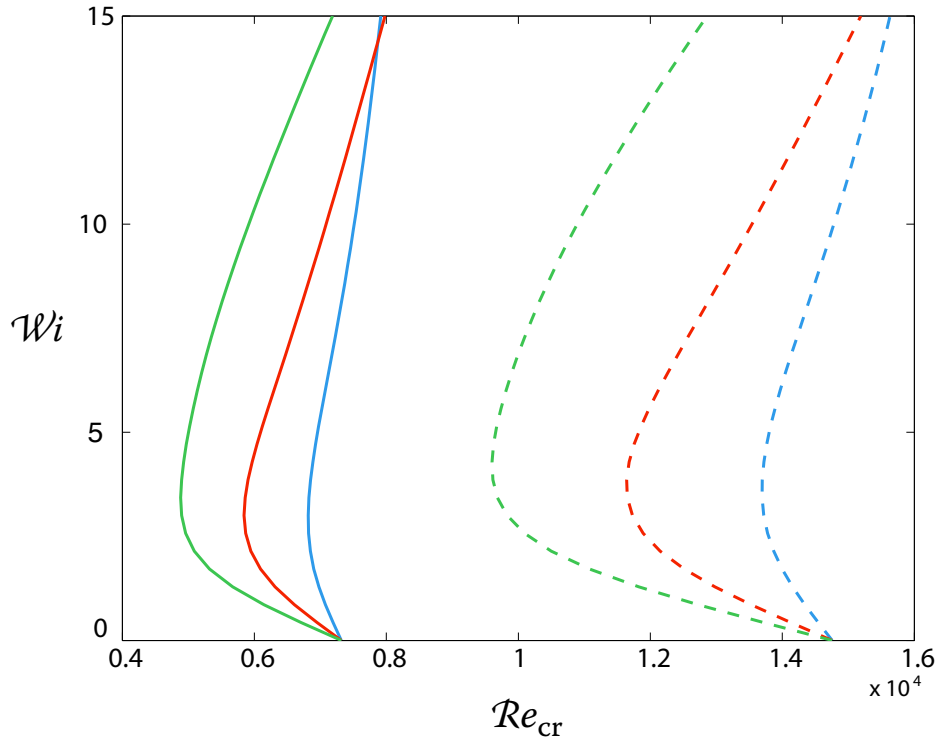
case so that all the curves start from zero. The curves corresponding to the same viscosity ratio β but to two different values of r_1 collapse in the same line for the smaller values of the Weissenberg number, indicating a similarity in the behaviour of the destabilizing effect of increasing $\mathcal{W}i$ with respect to r_2. However the minimum Reynolds number reached by the configuration closer to the circular pipe, i.e. $r_1 = 2$, is smaller and suggests a more *prominent* destabilizing effect of the Weissenberg number for the smaller values of r_1, even if the global effect of diminishing r_1 is to shift forward the critical Reynolds number of the Newtonian case and thus to *globally* stabilize the flow.

The introduction of a suitable Deborah number, $\mathcal{D}e = \omega_{r_{cr}} \mathcal{W}i$,[3] that compares the relaxation time to the real part of the frequency of the least stable eigenvalue leads to Figure 4.5 where $\mathcal{D}e$ is plotted as a function of the Reynolds number related to the polymer viscosity,

[3] B. Sadanandan and R. Sureshkumar (2002). "Viscoelastic effects on the stability of wall-bounded shear flows". In: *Physics of Fluids* 14.1, pp. 41–48.
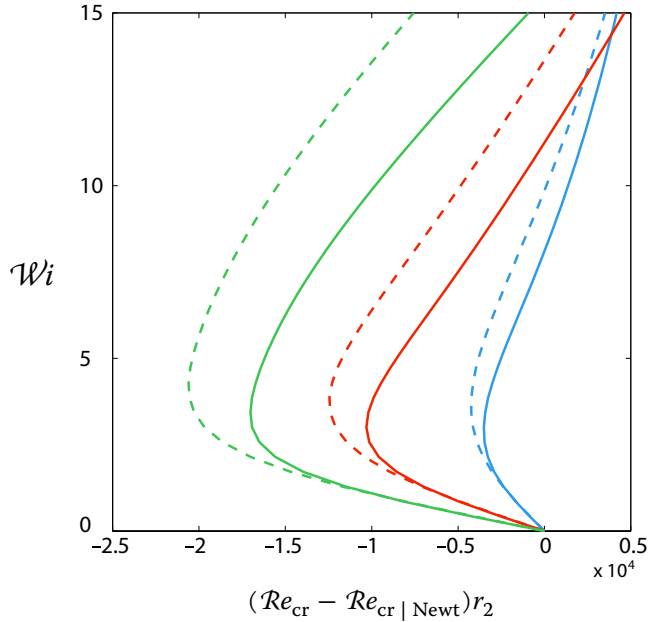
Figure 4.4: Effects of $\mathcal{W}i$ and β (● = 0.9, ● = 0.7, ● = 0.5) on $\mathcal{R}e_{cr}r_2$ of the APF for $r_1 = 5(-)$ and $r_1 = 2$ (– –)

$(\mathcal{R}e_{cr} - \mathcal{R}e_{cr\,|\,Newt})/(1-\beta)$. In this figure the minimum critical Reynolds number is reached for approximately unitary values of $\mathcal{D}e$. This indicates how the destabilizing effect of increasing the Weissenberg number occurs until the relaxation time is shorter than the characteristic time of the instability. Moreover the curves related to different value of the viscosity ratio β collapse in the same line for the smaller values of $\mathcal{D}e$. This is due to the choice of *modified* Reynolds number, $(\mathcal{R}e_{cr} - \mathcal{R}e_{cr\,|\,Newt})/(1-\beta)$, and implies a proportionality of the destabilizing effect with the polymer-induced viscosity.[4]

[4] Zhang et al., "Linear stability analysis of channel flow of viscoelastic Oldroyd-B and FENE-P fluids".

Non-axisymmetric disturbances must also be considered when the marginal curves are calculated since there is no analogue of Squire's theorem in the cylindrical geometry not even for the Newtonian case.

The critical Reynolds number, $\mathcal{R}e_{cr}$, is plotted as a function of the radii ratio, η, in Figure 4.6, while in Figure 4.7 the related streamwise wavenumbers, k_{cr}, for the axisymmetric disturbances, $m = 0$, is reported.
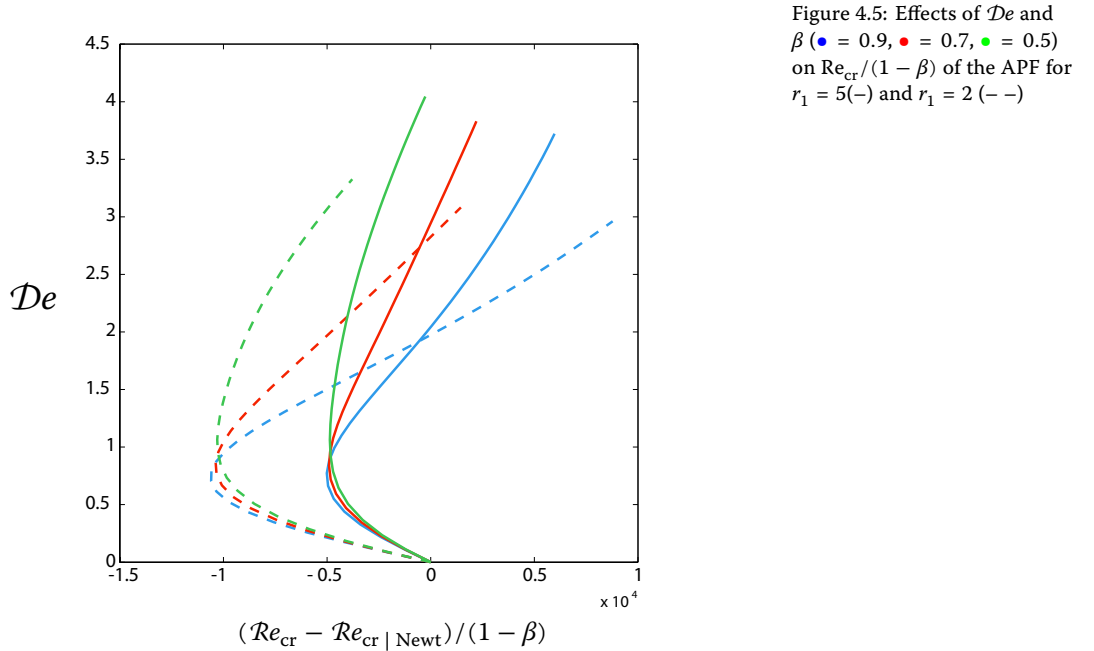
As it happens for the Newtonian case of APF[5] disturbances with $m \neq 0$ can be the cause of the marginal instability when moving from the planar channel case, $\eta = 1$, to the circular pipe; on the other hand, for the limit of η that tends to 1 the Squire's theorem has to be valid and in fact, even if it is not caught by the resolution of Figure 4.6, the asymptotic $\mathcal{R}e_{cr}$ for $\eta \rightarrow 1$ of disturbances with azimuthal wave number $m = 1$ is greater than the one of disturbances with $m = 0$.

Heaton, applying asymptotic arguments to the Newtonian case, extended previous results by Mott and Joseph and Cotrell and Pearlstein and demonstrated that that non-axisymmetric disturbances, i.e. $m \neq 0$, become stable at all $\mathcal{R}e$, i.e. $\mathcal{R}e_{cr}$ blows up to infinity, for finite values of the radii ratio η less than a certain value. In particular for disturbances with $m = 1$ there is a vertical asymptote for $\eta \cong 0.117$. For the case of $m = 0$ the asymptote is located at η that tends to zero implying that for $\eta < 0.117$ a finite critical Reynolds number exists.

Even if an extensive investigation on the presence of such asymptotes also for the viscoelastic case has not been conducted, Figure 4.6 suggests the also for the APF of Oldroyd-B fluids the same behaviour

[5] see Heaton, "Linear instability of annular Poiseuille flow".
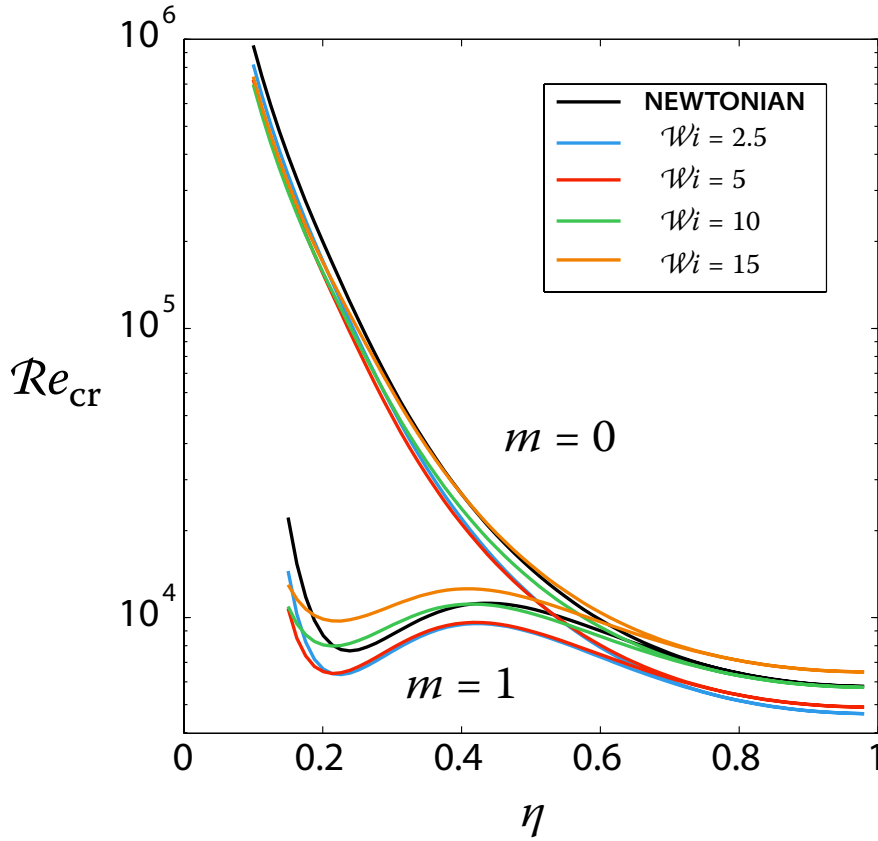
happens: a vertical asymptote seems to be located approximately at $\eta = 0.117$ for disturbances with unitary azimuthal wavenumber while for the axisymmetric disturbances the critical Reynolds numbers seems to go to infinity for $\eta \to 0$.

Kinetic Energy Analysis

The analysis of the budget of kinetic energy for the modal disturbances has been evaluated at various η and Wi for the critical values of Re and k. The azimuthal wavenumber m has been chosen depending on η as the most critical between $m = 0$ and $m = 1$ by using the results reported in Figure 4.6.
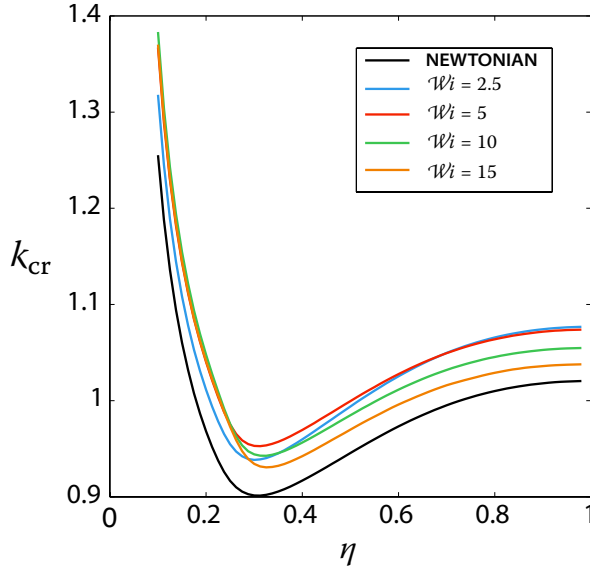
Figure 4.7: Effects of η on the critical streamwise wavenumber k_{cr} of the APF for $\beta = 0.7$, $m = 0$ and various values of $\mathcal{W}i$

The choice of the critical values of $\mathcal{R}e$ and k implies that

$$\dot{E}_K = I + D_v + W_p = 0 \qquad (4.1)$$

where the contributions to the kinetic energy budget are the Reynolds stress production, I, the viscous dissipation D_v and the polymer work W_p, as expressed by equation (3.26). In fact for $\mathcal{R}e_{cr}$, k_{cr} the imaginary part of the least stable eigenvalue is zero by definition then $\dot{E}_K = 0$ being valid the equivalence $\dot{E}_K = 2\omega_i$ for the modal case.

The viscosity ratio β has been chosen equal to 0.7 in all the computation while the Newtonian case has been obtained with both $\beta = 1$ and $\mathcal{W}i \to 0$ procedures.

The results for a value of the radii ration $\eta = 0.9$ near to the narrow gap limit are plotted in Figure 4.8 while some numerical results are reported in Table 4.1; for small values of $\mathcal{W}i$, the viscous dissipation D_v mainly compensates for the destabilizing effect of the Reynolds stress I while the negative work of the polymer plays a secondary role. On the other hand for $\mathcal{W}i = 15$ the Reynolds stress production is highly attenuated while the polymer stress is the main destabilizing cause that is offset by a great increase of the viscous dissipation.

In Figure 4.10 the results of the energy budget performed for $\eta = 0.2$ are graphed, while in Table 4.2 some numerical values are reported. As it can be seen by Figure 4.6, for this configuration the critical case is given by a disturbance with $m = 1$. In comparison with the previous case in which the most critical case was give by an axisymmetric disturbance the viscous dissipation D_v behave differently because firstly increases and after decreases with $\mathcal{W}i$ while the behaviour of the Reynolds stress production and polymer stress work remains the same.
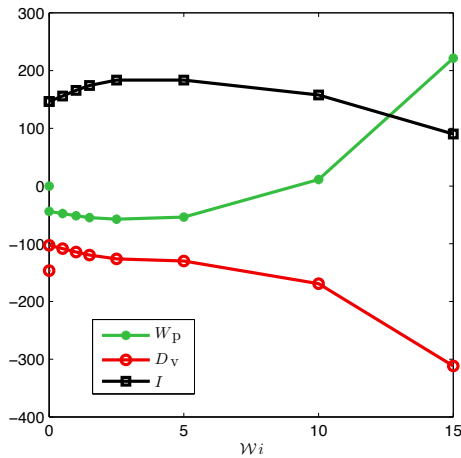
Figure 4.8: Kinetic energy analysis of APF $\eta = 0.9$ $\beta = 0.7$ for $\mathcal{R}e_{cr}$, k_{cr} and $m_{cr} = 0$. Note that all the terms have been multiplied by 10^4.
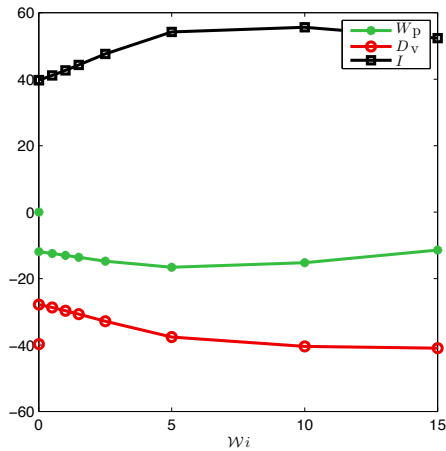
Figure 4.9: Kinetic energy analysis of APF $\eta = 0.1$ $\beta = 0.7$ for $\mathcal{R}e_{cr}$, k_{cr} and $m_{cr} = 0$. Note that all the terms have been multiplied by 10^4.
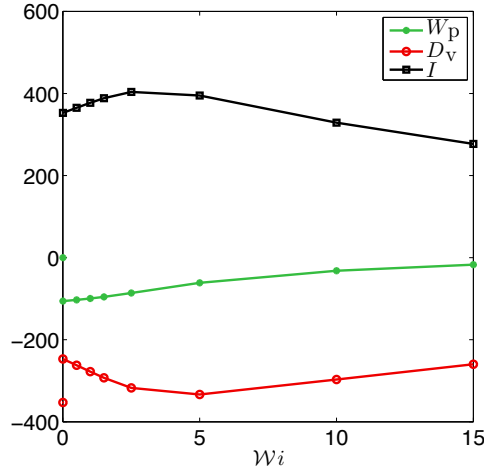
Figure 4.10: Kinetic energy analysis of APF $\eta = 0.2$ $\beta = 0.7$ for $\mathcal{R}e_{cr}$, k_{cr} and $m_{cr} = 1$. Note that all the terms have been multiplied by 10^4.

A PARTICULAR ATTENTION must be given to the Newtonian case. For the $\beta = 1$ case the polymer work is zero and only the viscous dissipation compensate for the Reynolds stress production. This is due to the decoupling of the governing equations related to the evolution of the conformation tensor from the ones related to the conservation of mass and the momentum balance. Moreover this implies that eigenvectors related to the latter equations will have zeros on the components of the conformation tensor. For the case of $\mathcal{W}i$ tending to zero there is no decoupling and then the eigenvectors do not *necessarily* have zero values for the conformation tensor components; thus more in general even if the eigenspectra for $\beta = 1$ and the ones for $\mathcal{W}i \to 0$ tend to coincide the eigenvectors do not.

However the polymer-contributed stress tensor behave as the viscous one and the following considerations on the Newtonian case obtained with both limits be made

- the total dissipation $D_v + W_p$ of the $\mathcal{W}i \to 0$ case coincide with the viscous dissipation of the $\beta = 1$ case

- both the total dissipation $D_v + W_p$ of the $\mathcal{W}i \to 0$ case and the viscous dissipation of the $\beta = 1$ case are equal in modulus to the Reynolds stress production I as a consequence of the choice of critical values

TERMS$\times 10^4$	Newt. $\beta = 1$	$\mathcal{W}i = 2.5$	$\mathcal{W}i = 5$	$\mathcal{W}i = 15$
W_p		-57.5233	-53.7181	221.4662
D_v	146.5444	-126.1754	-129.8034	-311.6306
I	146.5444	183.6987	183.5215	90.1288

Table 4.1: Kinetic energy analysis of APF $\eta = 0.9$ $\beta = 0.7$ for $\mathcal{R}e_{cr}$, k_{cr} and $m_{cr} = 0$

TERMS $\times 10^4$	Newt. $\beta = 1$	$\mathcal{W}i = 2.5$	$\mathcal{W}i = 5$	$\mathcal{W}i = 15$
W_p		-86.2732	-61.4777	-17.1622
D_v	-352.8304	-317.5215	-333.5614	-259.8976
I	352.8833	403.8632	395.1088	277.0844

Table 4.2: Kinetic energy analysis of APF $\eta = 0.2$ $\beta = 0.7$ for $\mathcal{R}e_{cr}$, k_{cr} and $m_{cr} = 1$

- in the $\mathcal{W}i \to 0$ case, the contribution of the polymer work to the total dissipation is given by the factor $1 - \beta$. An analogous proportion is valid for the viscous dissipation for which the factors.

These proportions, that are valid only for the limit of the Weissenberg number that tends to zero and do not apply when it increases, show how making the relaxation time tend to zero implies that the polymeric part of the stress acts in the same way as the viscous one. By this point of view the viscosity ratio β becomes merely a proportionality factor between two parts of the total stress tensor that act both in a Newtonian way.

NON-MODAL STABILITY ANALYSIS

Non-modal stability analysis has been performed by perturbing only the velocity vector and evaluating only its amplification. The amplification that the disturbances experience are relevant and comparable to the ones obtained for the Newtonian case. Some examples of $G(t)$ are graphed in Figure 4.11 for an oblique disturbance $k = 1.02$, $m = 2$, $\mathcal{R}e = 4000$, $\beta = 0.5$, $\eta = 0.3$ for two different values of the Weissenberg number $\mathcal{W}i = 2$ and $\mathcal{W}i = 15$ and compared with the Newtonian case $\beta = 1$.

In figure 4.12 the ratio, $G_{max}/G_{max|Newt}$ between the maximum growth for the Oldroyd-B fluid and the corresponding maximum growth for the Newtonian case is plotted for various values of the Weissenberg number $\mathcal{W}i$ and the viscosity ratio β. The effect of increasing the Weissenberg number on oblique disturbances is different from the impact on the quasi-planar ones. For the latter, i.e. for
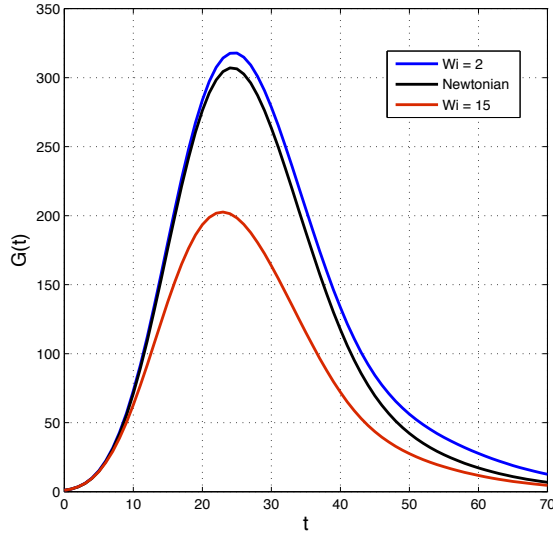
Figure 4.11: Growth function $G(t)$ for $\mathcal{R}e = 4000$, $\beta = 0.5$, $\eta = 0.3$, $m = 2$, $k = 1.02$ and two different values of $\mathcal{W}i$ compared to the Newtonian case

disturbances related to small values of k, augmenting $\mathcal{W}i$ makes the maximum growth increase monotonically. For oblique disturbances instead increasing the Weissenberg number affects the behaviour of $G_{\max}$ in a mixed way. In fact it firstly increases until a certain value of $\mathcal{W}i$ is reached and then decreases. The effect of decreasing the viscosity ratio, β, is to amplify the effects of the Weissenberg.

Kinetic energy budget may help to understand this two different behaviours. The optimal disturbance, i.e. the initial disturbance that reaches the maximum of the growth has been evaluated by mean of the Singular Value Decomposition, SVD, of the evolution operator defined with the filter matrices and the kinetic energy budget have been performed for various cases of the of the Weissenberg number and compared with the Newtonian case.

A first look must be given to the Newtonian case obtained starting from the Oldlroyd-B model either by putting β equal to one or by making the Weissenberg number tend to zero. The results for the kinetic energy analysis performed on the case with $\mathcal{R}e = 4000$, $k = 1.02$, $m = 2$ and $\beta = 0.7$ are graphed in Figure 4.13. The solid lines represent the case of $\mathcal{W}i \to 0$ while the circles are obtained for $\beta = 1$.
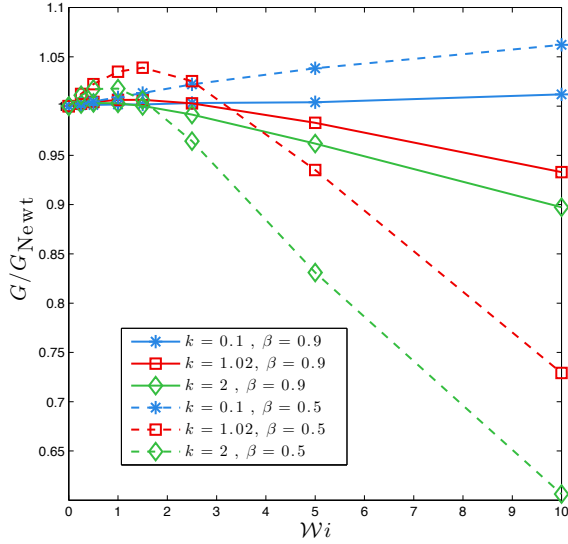
Figure 4.12: Maximum of the growth function G_{max} depending on the Weissenberg number, $\mathcal{W}i$, and the streamline wave number, k, for various values of the viscosity ratio, β

As it is possible to see from this figure, both the Reynolds stress production, I, and the overall kinetic energy time derivative, $\dot{E}_{\text{K}}$, are the same in both the $\mathcal{W}i \to 0$ and $\beta = 1$ cases.

Moreover, as it happens for the kinetic energy analysis performed on the modal disturbance, the viscous dissipation of the $\beta = 1$ case coincide with the total dissipation $W_{\text{p}} + D_{\text{v}}$ of the $\mathcal{W}i \to 0$ case. This time the proportionality factor given by $1 - \beta$ for the polymer work is extended to the overall evolution of this term, confirming that the polymer contribution actually behaves exactly as the viscous dissipation when the relaxation time is zero.

Increasing the Weissenberg number $\mathcal{W}i$ has the following general effects on oblique disturbances with respect to the Newtonian case

- the maximum of the Reynolds stress production I diminishes

- the minimum of the total dissipation diminishes in modulus and is reached in longer times

- the polymer work increases

The overall effect on the growth function is mixed and depends on the
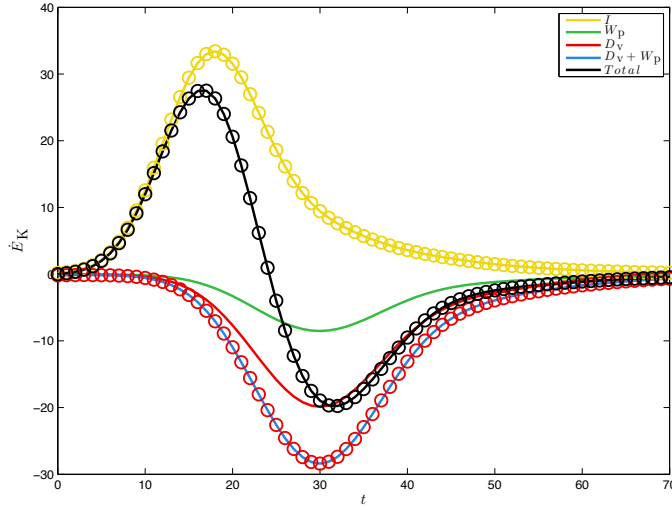
Figure 4.13: Non-modal kinetic energy analysis for an oblique disturbance (Newtonian case). $\mathcal{R}e = 4000$, $k = 1.02$, $m = 2$, $\eta = 0.3$; Newtonian case is obtained for either

– *solid lines* $\mathcal{W}i \to 0$ & $\beta = 0.7$

○ *circles* $\beta = 1$

Weissenberg number $\mathcal{W}i$, as it has been seen by Figure 4.12.

In order to explain the causes underlying the increase of the maximum of the growth function for oblique disturbances at low Weissenberg number, the kinetic energy analysis has been performed for $\mathcal{R}e = 4000$, $k = 1.02$, $m = 2$, $\beta = 0.5$, $\eta = 0.3$, and $\mathcal{W}i = 2$. The results are graphed (solid lines) in Figure 4.14 and are compare with the Newtonian case ($\beta = 1$, circles). Note that the red dashed line (– –) represents both the viscous dissipation and polymer work W_p for the Newtonian case obtained for $\mathcal{W}i \to 0$; they coincide because $\beta = 0.5$.

As it is possible to see, the total dissipative effect given by the sum of the viscous dissipation and the polymer work, $D_v + W_p$, diminishes with respect to the Newtonian case and compensates for the decrease of the maximum of the Reynolds stress production. In this case the reduction is due by the fact that the increase of the polymer work (the green line is above the dashed line) is not completely counteracted by the more prominent dissipative effect given by the solvent viscosity (the red line is beneath the the dashed line).

However the most important effect of the Weissenberg number is that the maximum of the absolute value of the total dissipation is reached in longer times compared to the Newtonian case. This is due
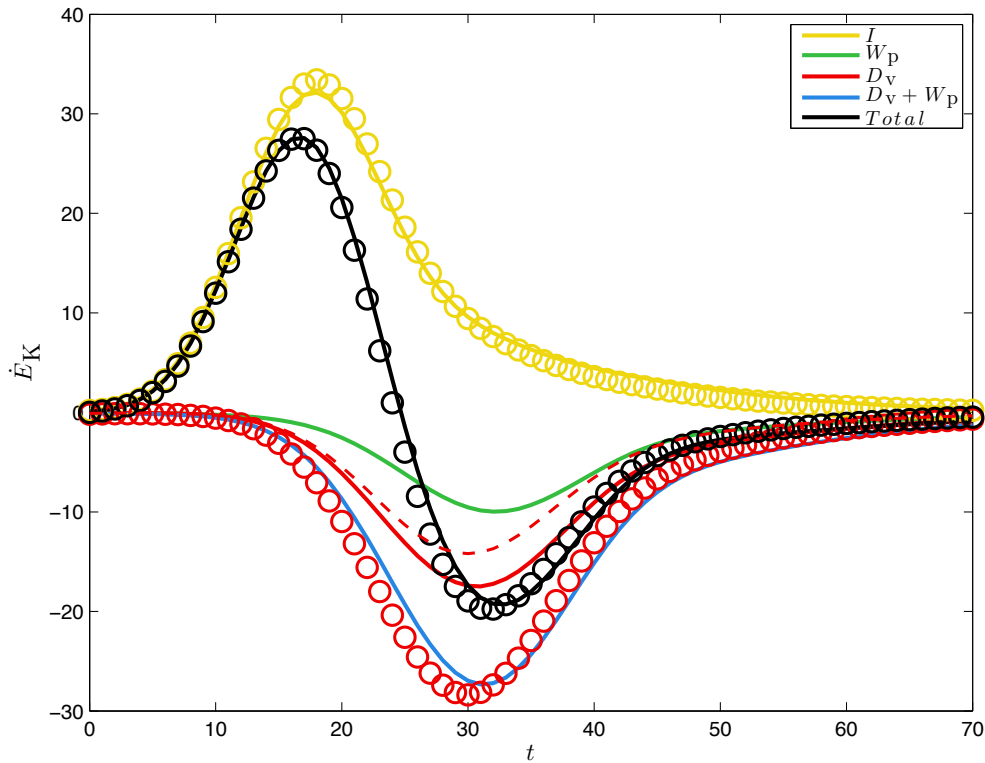
Figure 4.14: Non-modal kinetic energy analysis for an oblique disturbance.

– *solid lines* $\mathcal{R}e$ = 4000, k = 1.02, m = 2, β = 0.5, η = 0.3, $\mathcal{W}i$ = 2

○ *circles*   Newtonian case β = 1

– – *dashed line* $D_\mathrm{v} = W_\mathrm{p}$ Newtonian case $\mathcal{W}i \to 0$ & β = 0.5

to a shift forward of both the minimum of the viscous dissipation and the polymer work. In fact, while the compensation of the decrease of I, given by the drop of the dissipative effects, let the time derivative of the kinetic energy remain the same until the maximum is reached at $t \cong 17$, the retardation of the the dissipative effect maximum make the $\dot{E}_\mathrm{K}$ decrease (for $t > 17$) more slowly than in the Newtonian case, thus letting the growth function reach a greater maximum value.

The influence of the retardation effect on the total dissipation due to the increase of the Weissenberg number $\mathcal{W}i$ becomes less important when the reduction of the Reynolds stress production I becomes so predominant that can not be compensated by the increase of the polymer work on the fluid. In Figure 4.15 the results of the kinetic
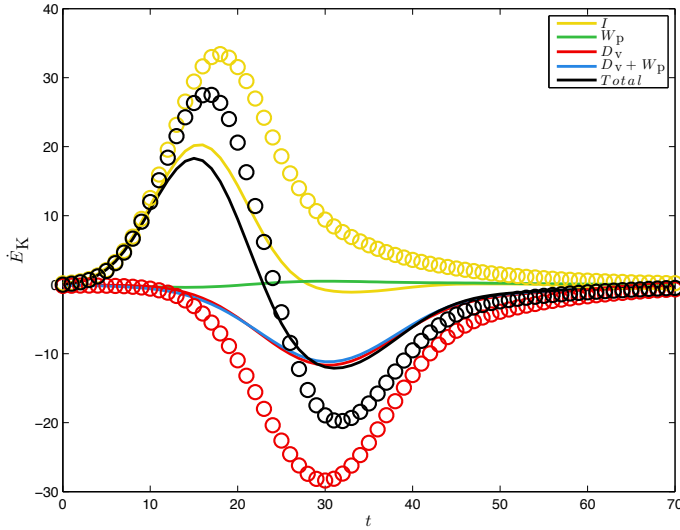
Figure 4.15: Non-modal kinetic energy analysis for an oblique disturbance.

– *solid lines* $\mathcal{R}e$ = 4000, k = 1.02, m = 2, β = 0.5, η = 0.3, $\mathcal{W}i$ = 15

○ *circles* Newtonian case β = 1

analysis performed on the case of $\mathcal{R}e$ = 4000, k = 1.02, m = 2, β = 0.5, η = 0.3 and $\mathcal{W}i$ = 15 are graphed. In this case the the decrease of the Reynolds stress production is so significant that not even the positive work made by polymer can counteract it. The overall effect is then a reduction the growth function maximum.

The monotonic increase of the maximum value of the growth function, G_{max}, on the quasi-planar disturbances due to augmenting the Weissenberg number, $\mathcal{W}i$, can be explained with a different mechanism than the one shown for oblique disturbances. The results of the kinetic energy analysis on the case with $\mathcal{R}e$ = 4000, k = 0.1, m = 2, β = 0.5, η = 0.3, $\mathcal{W}i$ = 5 are plotted in Figure 4.16. As it has been seen for oblique disturbances, the polymer work increases and the viscous dissipation decreases with respect to the Newtonian case ($\mathcal{W}i \rightarrow 0$, – – dashed line). Even if this fact does not significantly affect the absolute value of the maximum of the total dissipation and neither its position, it is important for the amount of dissipation in the first time steps that is reduced with respect to the Newtonian case. Adding this effect to the fact that the Reynolds stress production grows faster makes the time derivative of the kinetic energy reach a greater
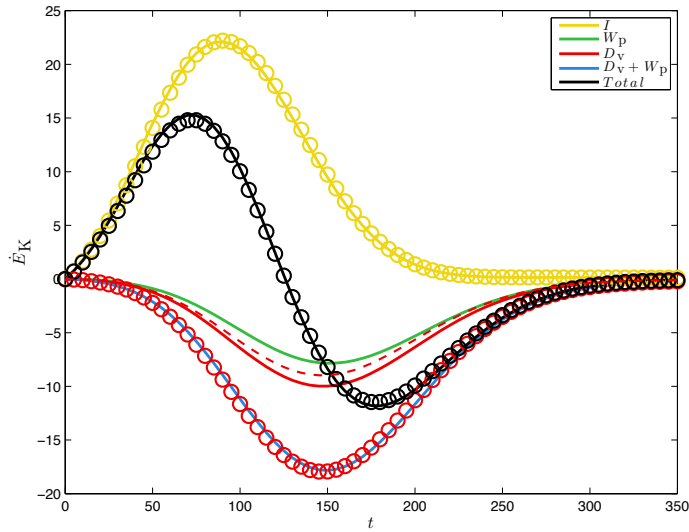
Figure 4.16: Non-modal kinetic energy analysis for an oblique disturbance.

– *solid lines* $\mathcal{Re} = 4000$, $k = 0.1$, $m = 2$, $\beta = 0.5$, $\eta = 0.3$, $\mathcal{Wi} = 5$

○ *circles* Newtonian case $\beta = 1$

– – *dashed line* $D_v = W_p$ Newtonian case $\mathcal{Wi} \to 0$ & $\beta = 0.5$

maximum than the Newtonian case. The overall effect is then that the growth function maximum increases.

5

CONCLUSIONS

The linear stability of inertia dominated shear flows in pipes of highly
dilute polymer solution has been performed. The Oldroyd-B model
has been chosen as the constitutive equation for describing the
behaviour of the stress tensor of these fluids.

A preliminary study has been carried out on the *state of the art*
of the mathematical tools used for the linear stability analysis, in
particular the non-modal one, and some new ideas has been presented.
In fact, the mathematical framework is such as to prevent a straightforward
use of the non-modal stability analysis as proposed for the incompressible
Newtonian case and this is one of the reasons why papers focusing on
this kind of analysis appeared only recently.

They dealt exclusively with the channel flow configuration while in
this work the annular flow has been extensively studied. The cylindrical
geometry is more interesting than the more academic planar configuration
also by an industrial and applicative point of view but presents further
problems of both mathematical and numerical nature that have been
faced up in order to deal with it.

The main results obtained are related to the effects of the Weissenberg
number and the curvature of the annular geometry on the characteristic
of the modal stability of the flow. The critical Reynolds number
exhibits the characteristic non-monotonic behaviour depending on
the Weissenberg number and the overall effect of tending to the pipe
is to modally stabilize the flow. However the destabilizing effect of
the Weissenberg number with respect to the Newtonian case is more
prominent when the geometry tends to the pipe.

The non-modal stability analysis has been carried out by taking into account perturbations of the velocity vector only and monitoring only its amplifications. The effect of the Weissenberg number is to increase the maximum amplification of quasi-planar disturbances. The effect on oblique disturbances is instead non-monotonic, i.e. there is a maximum after which further increases of the Weissenberg number lead to a drop in the amplification. This behaviour has been investigated by means of the kinetic energy analysis.

The damping of the maximum amplification for oblique disturbances at high Weissenberg number can be simply explained by the drop of the Reynolds stress production. An analogous motivation is related to the increase of the maximum amplification for quasi-planar disturbance at the same values of the Weissenberg number: the greater amplification is due to an increase of the Reynolds stress production. Instead, the increase of the maximum amplification at intermediate values of the Weissenberg number for oblique disturbances is related to different mechanisms. In this case the main role is played by the timing of the productive and dissipative effects, that are both damped by the action of the Weissenberg number. The greater amplification is due to a shift forward of the time at which the dissipative effect reaches its peak.

A

LINEAR OPERATORS

The projection of (3.6) and (3.7) to the chosen system of reference leads to

$$0 = \left(\frac{\partial}{\partial r} + \frac{1}{r}\right)\tilde{u} + \mathrm{i}\frac{m}{r}\tilde{v} + \mathrm{i}k\tilde{w} \tag{A.1}$$

$$-\mathrm{i}\omega\tilde{u} = \left[-\mathrm{i}k\overline{W} + \frac{\beta}{\mathcal{R}e}\left(\frac{\partial^2}{\partial r^2} + \frac{1}{r}\frac{\partial}{\partial r} - \frac{m^2+1}{r^2} - k^2\right)\right]\tilde{u} - 2\mathrm{i}\frac{\beta}{\mathcal{R}e}\frac{m}{r^2}\tilde{v} - \frac{\partial p}{\partial r}$$
$$+ \frac{1-\beta}{\mathcal{R}e\,\mathcal{W}i}\left[\left(\frac{1}{r} + \frac{\partial}{\partial r}\right)\tilde{c}_{rr} + \mathrm{i}\frac{m}{r}\tilde{c}_{r\theta} + \mathrm{i}k\tilde{c}_{rz} - \frac{\tilde{c}_{\theta\theta}}{r}\right] \tag{A.2}$$

$$-\mathrm{i}\omega\tilde{v} = 2\mathrm{i}\frac{\beta}{\mathcal{R}e}\frac{m}{r^2}\tilde{u} + \left[-\mathrm{i}k\overline{W} + \frac{\beta}{\mathcal{R}e}\left(\frac{\partial^2}{\partial r^2} + \frac{1}{r}\frac{\partial}{\partial r} - \frac{m^2+1}{r^2} - k^2\right)\right]\tilde{v} - \mathrm{i}\frac{m}{r}\tilde{p}$$
$$+ \frac{1-\beta}{\mathcal{R}e\,\mathcal{W}i}\left[\left(\frac{2}{r} + \frac{\partial}{\partial r}\right)\tilde{c}_{r\theta} + \mathrm{i}\frac{m}{r}\tilde{c}_{\theta\theta} + \mathrm{i}k\tilde{c}_{\theta z}\right] \tag{A.3}$$

$$-\mathrm{i}\omega\tilde{w} = -\overline{W}'\tilde{u} + \left[-\mathrm{i}k\overline{W} + \frac{\beta}{\mathcal{R}e}\left(\frac{\partial^2}{\partial r^2} + \frac{1}{r}\frac{\partial}{\partial r} - \frac{m^2}{r^2} - k^2\right)\right]\tilde{w} - \mathrm{i}k\tilde{p}$$
$$+ \frac{1-\beta}{\mathcal{R}e\,\mathcal{W}i}\left[\left(\frac{1}{r} + \frac{\partial}{\partial r}\right)\tilde{c}_{rz} + \mathrm{i}\frac{m}{r}\tilde{c}_{\theta z} + \mathrm{i}k\tilde{c}_{zz}\right] \tag{A.4}$$

and of (3.8) leads to

$$-i\omega\tilde{c}_{rr} = 2\left(\frac{\partial}{\partial r} + i\mathcal{W}i\overline{W}'k\right)\tilde{u} - \left(i\overline{W}k + \frac{1}{\mathcal{W}i}\right)\tilde{c}_{rr} \tag{A.5}$$

$$-i\omega\tilde{c}_{r\theta} = i\frac{1}{r}m\tilde{u} + \left(\frac{\partial}{\partial r} - \frac{1}{r} + i\mathcal{W}i\overline{W}'k\right)\tilde{v} - \left(i\overline{W}k + \frac{1}{\mathcal{W}i}\right)\tilde{c}_{r\theta} \tag{A.6}$$

$$-i\omega\tilde{c}_{rz} = \left\{\mathcal{W}i\overline{W}'\frac{\partial}{\partial r} - \mathcal{W}i\frac{\partial^2\overline{W}}{\partial r^2} + i\left[1 + 2\mathcal{W}i^2\left(\overline{W}'\right)^2\right]k\right\}\tilde{u} + \left(\frac{\partial}{\partial r} + i\mathcal{W}i\overline{W}'k\right)\tilde{w}$$
$$+ \overline{W}'\tilde{c}_{rr} - \left(i\overline{W}k + \frac{1}{\mathcal{W}i}\right)\tilde{c}_{rz} \tag{A.7}$$

$$-i\omega\tilde{c}_{\theta\theta} = \frac{2}{r}\tilde{u} + i\frac{2}{r}m\tilde{v} - \left(i\overline{W}k + \frac{1}{\mathcal{W}i}\right)\tilde{c}_{\theta\theta} \tag{A.8}$$

$$-i\omega\tilde{c}_{\theta z} = \left\{\mathcal{W}i\overline{W}'\frac{\partial}{\partial r} - \frac{\mathcal{W}i}{r}\overline{W}' + i\left[1 + 2\mathcal{W}i^2\left(\overline{W}'\right)^2\right]k\right\}\tilde{v} + i\frac{1}{r}m\tilde{w} + \overline{W}'\tilde{c}_{r\theta}$$
$$- \left(i\overline{W}k + \frac{1}{\mathcal{W}i}\right)\tilde{c}_{\theta z} \tag{A.9}$$

$$-i\omega\tilde{c}_{zz} = -4\mathcal{W}i^2\overline{W}'\overline{W}''\tilde{u} + 2\left\{\mathcal{W}i\overline{W}'\frac{\partial}{\partial r} + i\left[1 + 2\mathcal{W}i^2\left(\overline{W}'\right)^2\right]k\right\}\tilde{w} + 2\overline{W}'\tilde{c}_{rz}$$
$$- \left(i\overline{W}k + \frac{1}{\mathcal{W}i}\right)\tilde{c}_{zz} \tag{A.10}$$

BIBLIOGRAPHY

Ash, R. L. and M. R. Khorrami (1995). "Vortex Stability in *Fluid Vortices*". In: Kluwer, pp. 317–372.

Balci, N. et al. (2011). "Symmetric factorization of the conformation tensor in viscoelastic fluid models". In: *Journal of Non-Newtonian Fluid Mechanics* 166.11, pp. 546–553.

Bird, R. B. and J. M. Wiest (1995). "Constitutive equations for polymeric liquids". In: *Annual review of fluid mechanics* 27.1, pp. 169–193.

Bird, R.B., R. C. Armstrong, and O. Hassager (1987a). *Dynamics of Polymeric Liquids. Fluid Mechanics*. Second Edition. Vol. I. Wiley-Iterscience.

Bird, R.B. et al. (1987b). *Dynamics of Polymeric Liquids. Kinetic Theory*. Second Edition. Vol. II. Wiley-Iterscience.

Boyd, J. P. (2000). *Chebyshev and Fourier spectral methods*. Second Edition. Dover Publications.

Cotrell, D. L. and A. J. Pearlstein (2006). "Linear stability of spiral and annular Poiseuille flow for small radius ratio". In: *Journal of Fluid Mechanics* 547, pp. 1–20.

Doering, C. R., B. Eckhardt, and J. Schumacher (2006). "Failure of energy stability in Oldroyd-B fluids at arbitrarily low Reynolds numbers". In: *Journal of Non-Newtonian Fluid Mechanics* 135.2, pp. 92–96.

Flory, P. J. (1969). *Statistical mechanics of chain molecules*. Wiley-Interscience.

Giesekus, H. (1982). "A simple constitutive equation for polymer fluids based on the concept of deformation-dependent tensorial mobility". In: *Journal of Non-Newtonian Fluid Mechanics* 11.1, pp. 69–109.

Hanifi, A., P. J. Schmid, and D. S. Henningson (1996). "Transient growth in compressible boundary layer flow". In: *Physics of Fluids* 8.3, pp. 826–837.

Heaton, C. J. (2008). "Linear instability of annular Poiseuille flow". In: *Journal of Fluid Mechanics* 610, pp. 391–406.

Ho, T. C. and M. M. Denn (1977). "Stability of plane Poiseuille flow of a highly elastic liquid". In: *Journal of Non-Newtonian Fluid Mechanics* 3.2, pp. 179–195.

Hoda, N., M. R. Jovanović, and S. Kumar (2008). "Energy amplification in channel flows of viscoelastic fluids". In: *Journal of Fluid Mechanics* 601, pp. 407–424.

– (2009). "Frequency responses of streamwise-constant perturbations in channel flows of Oldroyd-B fluids". In: *Journal of Fluid Mechanics* 625, pp. 411–434.

James, D. F. (2009). "Boger Fluids". In: *Annual review of fluid mechanics* 41, pp. 129–142.

Jovanović, M. R. and S. Kumar (2010). "Transient growth without inertia". In: *Physics of Fluids* 22.2, p. 023101.

– (2011). "Nonmodal amplification of stochastic disturbances in strongly elastic channel flows". In: *Journal of Non-Newtonian Fluid Mechanics* 166.14, pp. 755–778.

Khorrami, M. R., M. R. Malik, and R. L. Ash (1989). "Application of spectral collocation techniques to the stability of swirling flows". In: *J. Comp. Phys.* 81, pp. 206–229.

Larson, R. G. (1992). "Instabilities in viscoelastic flows". In: *Rheologica Acta* 31.3, pp. 213–263.

– (1999). *The Structure and Rheology of Complex fluids*. Oxford University Press, New York.

Lozinski, A. and R. G. Owens (2003). "An energy estimate for the Oldroyd B model: theory and applications". In: *Journal of Non-Newtonian Fluid Mechanics* 112.2, pp. 161–176.

Meulenbroek, B. et al. (2004). "Weakly nonlinear subcritical instability of visco-elastic Poiseuille flow". In: *Journal of Non-Newtonian Fluid Mechanics* 116, pp. 235–268.

Mott, J. and D. Joseph (1968). "Stability of parallel flow between concentric cylinders". In: *Physics of Fluids* 11.10.

Oldroyd, J. G. (1950). "On the Formulation of Rheological Equations of State". In: *Proceedings of the Royal Society of London A: Mathematical, Physical and Engineering Sciences* 200.1063, pp. 523–541.

Phan-Thien, N. (2012). *Understanding Viscoelasticity*. Springer.

Porteous, K. C. and M. M. Denn (1972). "Linear stability of plane Poiseuille flow of viscoelastic liquids". In: *Transactions of The Society of Rheology (1957-1977)* 16.2, pp. 295–308.

Rallison, J. M. and E. J. Hinch (1988). "Do we understand the physics in the constitutive equation?" In: *Journal of Non-Newtonian Fluid Mechanics* 29, pp. 37–55.

Sadanandan, B. and R. Sureshkumar (2002). "Viscoelastic effects on the stability of wall-bounded shear flows". In: *Physics of Fluids* 14.1, pp. 41–48.

Schmid, P. J. (2007). "Nonmodal Stability Theory". In: *Annu. Rev. Fluid Mech.* 39, pp. 129–162.

Schmid, P. J. and D. S. Henningson (1994). "Optimal energy density growth in Hagen-Poiseuille flow". In: *J. Fluid Mech.* 277, pp. 197–225.

– (2001). *Stability and transition in shear flow*. Springer.

Sureshkumar, R. and A. N. Beris (1995). "Linear stability analysis of channel flow of viscoelastic Oldroyd-B and FENE-P fluids". In: *Journal of Non-Newtonian Fluid Mechanics* 56, pp. 151–182.

Trefethen, L. N. and M. Embree (2005). *Spectra and pseudospectra: the behavior of nonnormal matrices and operators*. Princeton University Press, pp. xviii + 606.

Wilson, H. J., M. Renardy, and Y. Renardy (1999). "Structure of the spectrum in zero Reynolds number shear flow of the UCM and Oldroyd-B liquids". In: *Journal of Non-Newtonian Fluid Mechanics* 80.2, pp. 251–268.

Zhang, M. et al. (2013). "Linear stability analysis of channel flow of viscoelastic Oldroyd-B and FENE-P fluids". In: *Journal of Fluid Mechanics* 737, pp. 249–279.